Spring 1-1-2013

Medium-Pressure UV Disinfection: Evaluation of Unintended DNA Damage Reversal and Adenoviral Protein Damage Using Wavelength Specific Irradiation

Christopher Poepping
University of Colorado at Boulder, chris.poepping@gmail.com

Medium-Pressure UV Disinfection: Evaluation of Unintended DNA Damage Reversal and Adenoviral Protein Damage Using Wavelength Specific Irradiation

by

Christopher Poepping

B.S., Montana State University 2010

A thesis submitted to the Faculty of the Graduate School of the University of Colorado in partial fulfillment of the requirements for the degree of:

Master of Science

Department of Civil, Environmental, and Architectural Engineering

2013

This thesis entitled:

Medium-Pressure UV Disinfection: Evaluation of Unintended DNA Damage Reversal and Adenoviral Protein Damage Using Wavelength Specific Irradiation

written by Christopher Poepping

has been approved for the

Department of Civil, Environmental, and Architectural Engineering

_____

Karl G. Linden

_____

Roberto Rodriguez

_____

Fernando Rosario-Ortiz

August 16, 2013

The final copy of this thesis has been examined by the signatories, and we find that both the content and the form meet acceptable presentation standards of scholarly work in the above mentioned discipline.

Abstract

Poepping, Christopher

Medium-Pressure UV Disinfection: Evaluation of Unintended DNA Damage Reversal and Adenoviral Protein Damage Using Wavelength Specific Irradiation

Thesis directed by Professor Karl Linden

Medium-pressure (MP) ultraviolet (UV) lamps are becoming a popular technology for UV disinfection. They have demonstrated significant advantages over conventional low-pressure (LP) UV lamps including markedly increased inactivation efficiency for adenovirus, which is considered the most UV resistant pathogen. MP UV lamps produce a polychromatic emission throughout the UV spectrum compared to the monochromatic emission at 253.7 nm produced by LP UV lamps. With increased use of MP UV lamps comes a need to better understand the technology for regulatory and optimization purposes.

This research aims to increase the understanding of microbial inactivation and cellular damage resulting from polychromatic UV emission. It focuses on UV-induced damage resulting from single-wavelength exposures either alone or sequentially. DNA damage induced by UV light in the upper end of the UV-C spectrum, ~280 nm, has been shown to be directly reversible through subsequent irradiation at lower wavelengths, ~230-240 nm. Polychromatic emission allows for the possibility that DNA will be exposed to multiple wavelengths throughout the UV-C spectrum; therefore, there exists the possibility that some UV-induced damage may be inadvertently reversed during MP UV irradiation. It is important to know whether typical MP UV doses emit enough low-wavelength radiation to effectively reverse DNA damage as the technology would not be fully optimized if damage reversal is occurring. This was studied using culture techniques to examine cell viability and a quantitative polymerase chain reaction (qPCR)

to assess DNA damage. Multiple-wavelength exposures resulted in higher inactivation levels than single-wavelength exposures when using culture techniques for bacterial growth. However, DNA damage investigated through qPCR assays showed a significant decrease for samples subjected to multiple-wavelengths in sequence.

Single wavelength exposures were also used to investigate the causes for adenoviral resistance to LP UV irradiation and susceptibility to MP UV exposure. The mechanism responsible for increased inactivation efficiency by MP sources was studied through examining adenoviral protein damage resulting from single-wavelength exposures throughout the UV-C spectrum. This work helps to elucidate why MP UV lamps are so much more effective against adenovirus and also helps to understand the adenoviral mechanism responsible for its extreme resistance to LP UV irradiation. Protein damage was studied using sodium dodecyl sulfate – polyacrylamide gel electrophoresis (SDS-PAGE) as a means to separate and subsequently quantify protein presence. Initial results show significant protein damage at lower wavelengths, less than 230 nm, compared to the higher wavelengths in the UV-C spectrum.

Contents

List of Tables

List of Figures

1. Introduction

1.1 Low and Medium Pressure UV Lamps

Low-pressure (LP) and medium-pressure (MP) ultraviolet (UV) lamps are efficient and effective treatments for the inactivation of microorganisms. These technologies are widely used across public and private water treatment systems as a means for disinfection. LP UV disinfection systems have been around longer and have been generally considered as the prominent UV technology for disinfection purposes; however, in the last decade, MP UV systems have gained more attention and popularity as they have shown increased effectiveness against many microbes and challenge pathogens. The difference between the two lamps lies in their emission spectrum: LP UV lamps emit a monochromatic spectrum at 253.7 nm and MP UV systems produce a polychromatic emission spanning the UV spectrum (Figure 1-1). Recent research has shown a dramatic increase in the susceptibility of some pathogenic microbes, specifically adenovirus, to MP UV irradiation compared to that of LP UV irradiation, including some viruses which have typically been a challenge to UV disinfection practices (Linden et al., 2007; Guo et al., 2009; Linden et al., 2009; Shin et al., 2009; Guo et al., 2010; Rodríguez et al., 2013).

These observations have spurred increased implementation and optimization of MP UV lamps; however, this has birthed several issues regarding use. These issues include complex implementation and regulation stemming from different UV absorbance through the UV spectrum leading to difficult UV sensing capabilities and dose determination. Since LP UV lamps have been the method of choice for the UV community in the past, most mandated regulations and guidance manuals were developed based on LP UV requirements. Further, MP

UV technology advancement has given rise to a challenge known as the low wavelength issue, which is a result of low wavelength emission of MP UV lamps and the incorrect UV sensing and subsequent dose determinations at those wavelengths. This issue will be discussed in more detail later in the report. In addition to the challenges faced with the regulations and technology of MP UV lamps, there is still a lack of understanding regarding polychromatic emission and the specific mechanism of increased effectiveness of MP UV for certain microbes.

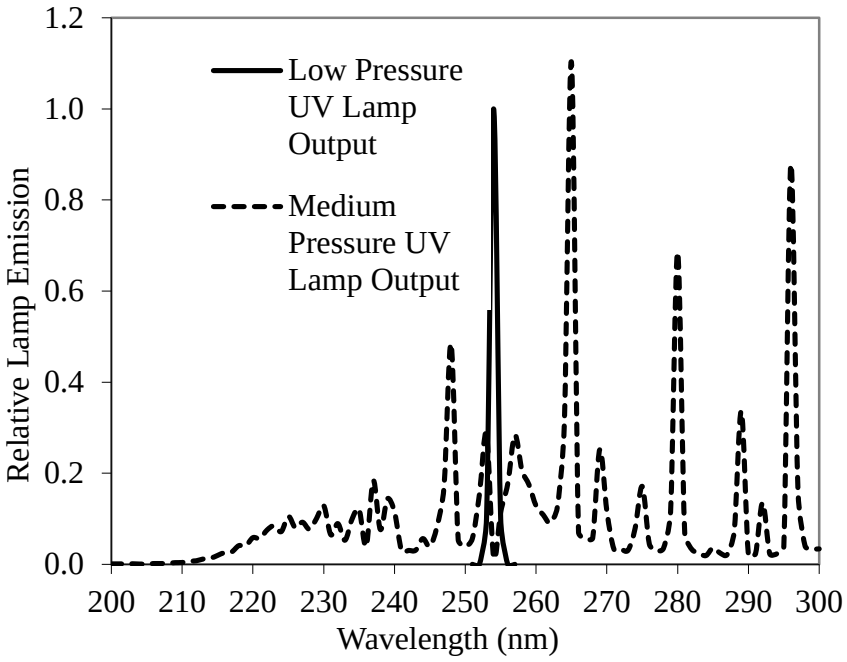

Figure 1-1: LP and MP UV lamp emissions

The overall aim of this research is to investigate aspects of MP UV irradiation through methods examining damage resulting from polychromatic emission at the molecular level. Specifically, two different aspects of polychromatic UV induced damage will be considered:

1.) The possibility for unintended DNA damage reversal resulting from multiple wavelength exposure as a result of polychromatic UV emission.

2.) An investigation of adenovirus inactivation resulting from MP UV irradiation using two different approaches. One approach compiled published data concerning MP UV adenovirus

inactivation and analyzed the compilation. Also, adenoviral protein damage as a result of wavelength-specific irradiation was investigated. This research will provide insight into a variety of elements concerning MP UV irradiation including regulatory aspects and more knowledge/exploration-based aspirations.

1.2 Thesis Organization

This thesis will be organized into separate chapters each with separate background, materials and methods, results, and discussion sections. Chapter 1 gives a short introduction into the objectives of the research and provides some background regarding the nature of UV light and necessary information. Chapter 2 discusses DNA damage and the potential for unintended damage reversal as a side effect of polychromatic emission. Chapter 3 discusses adenovirus and its effect on UV disinfection processes. Chapter 3 also contains an investigation involving wavelength-specific adenoviral protein damage. The appendix holds certain data and information on testing that was performed or considered during the research but not present in the thesis body.

1.3 UV Spectrum

The UV spectrum spans the range from 200-400 nm and this range is broken into three categories. UV-A light is considered to be the range of 320-400 nm. The UV-B range is 280-320 nm and the UV-C range is 200-280 nm. Solar UV-A and UV-B light can reach the surface of the earth and are the main culprits of skin cancers. Solar UV-C is filtered out by the atmosphere and does not reach the earth's surface; however, it is the most important category for disinfection purposes as it imparts the most damage to nucleic acids. LP UV lamps emit monochromatic light at 253.7 nm while MP UV emit polychromatic light spanning all three categories. UV induced

damage will be discussed in greater detail later.

1.4 Beer Lambert Law of Absorption

Light can be absorbed passing through various types of media including water. As a result, UV absorbance is an important aspect of disinfection as more absorbing mediums will result in less UV light available for proper disinfection. Light absorbance follows the Beer-Lambert law:

$$\log A = log\frac{I_0}{I} = \alpha \times z \times c \quad 1.$$

In the equation, A is the absorbance, I_0 is the intensity of light entering the sample, and I is the intensity of the light passing through the sample. Also, α is the molar absorption coefficient (M^{-1} cm^{-1}), z is the depth of the sample or the pathlength (cm), and c is the concentration of dissolved materials (M). UV transmittance (UVT) is used as a measure of the percentage of UV light passing through the sample and is described as:

$$UVT = 100 \times 10^{-A} \quad 2.$$

2. Unintended DNA Damage Reversal in MP UV Disinfection

2.1 Introduction

2.1.1 UV Induced DNA Damage

The foundation of UV disinfection lies in the ability of UV light to induce damage to DNA leading to inhibition of vital cellular processes such as transcription and replication and ultimately lead to the inactivation of the organism (Moné et al., 2001; Sinha and Häder, 2002;

Eischeid et al., 2011; Government, 2011; Rodríguez et al., 2013). As shown in the DNA absorption curve in Figure 2-1, DNA strongly absorbs UV-C (200-290 nm) with a relative peak at 260 nm.

Absorption of UV photons by DNA nucleobases can lead to excitation of these bases resulting in possible interactions between neighboring bases. Interactions primarily take place between neighboring pyrimidine bases, predominantly thymine. Although purine-pyrimidine and purine-purine interactions are possible, the amount is insignificant compared to interactions between pyrimidine bases (Ravanat et al., 2001; Cadet et al., 2005; Yates et al., 2006; Eischeid et al., 2011).

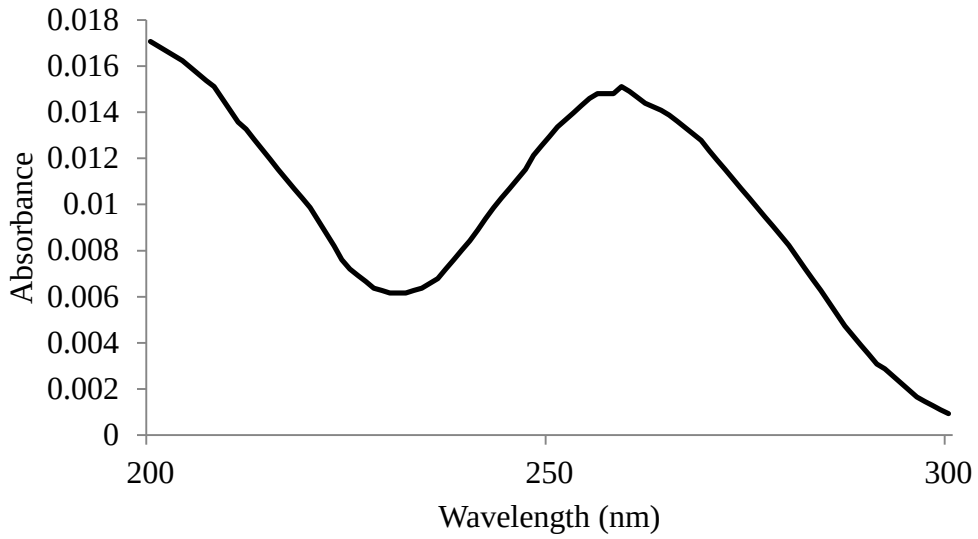

Figure 2-1: DNA absorption curve

These interactions can lead to the formation of lesions between the neighboring bases whose presence effectively disrupts vital cell machinery responsible for cellular transcription and replication processes. Two principle types of lesions can form between the bases: cyclobutane pyrimidine dimers (CPDs) and 6-4 photoproducts (Sinha and Häder, 2002; Linden et al., 2007;

Shin et al., 2009; Guo et al., 2010). Their structures are shown in Figure 2-2. CPDs are characterized as a four-membered ring structure with two carbon atoms on each base and 6-4 photoproducts are the characterized by a non-cyclic interaction between one carbon on each base (Yates et al., 2006; Rastogi et al., 2010; Eischeid and Linden, 2011). CPDs account for the majority of lesions induced by UV-C light comprising about 75% of lesions formed while the remaining 25% are 6-4 photoproducts (Sinha and Häder, 2002; Eischeid et al., 2011).

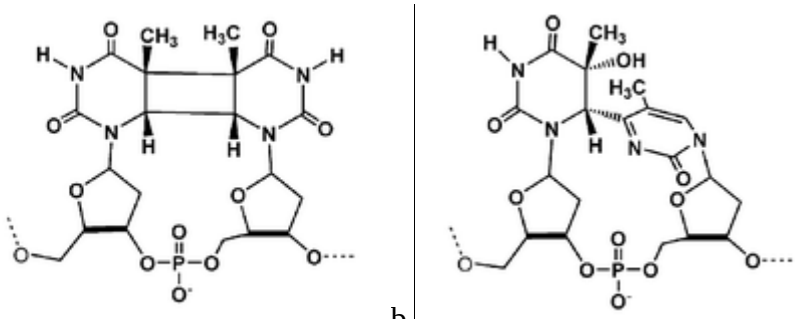

a. b.

Figure 2-2: Chemical structure of a.) cyclobutane pyrimidine dimer (CPD) and b.) 6-4 photoproduct. Both interactions take place between two neighboring thymine bases

2.1.2 Enzyme Mediated Repair Mechanisms

Many microbes have evolved mechanisms to repair UV-induced damage creating a major concern for UV disinfection processes. These mechanisms have been studied extensively and are well understood. There are two principal categories of DNA damage repair: photoreactivation and excision repair. Photoreactivation is an enzyme-mediated mechanism stimulated by the exposure to visible, near-UV light. Excision repair is also an enzyme-mediated mechanism but does not require visible light. Rather excision repair utilizes enzymes to directly remove damaged bases or nucleotide sequences and subsequently replace the removed parts with new undamaged components (Greber et al., 1993; Sinha and Häder, 2002; Zimmer and Slawson, 2002; Eischeid et al., 2011).

2.1.3 Direct Photoreversal of DNA Damage

In addition to enzyme-mediated DNA repair mechanisms, there has been evidence that UV-induced lesions can be directly cleaved through subsequent UV-C exposure. This direct photoreversal is independent of the enzyme-mediated processes listed above and is a direct result of photo-induced reactions. Past studies observed CPDs formed via irradiation at higher UV-C wavelengths, ~280 nm, can be directly cleaved, or split back to its original components, with subsequent irradiation from lower wavelength UV-C light around 240 nm (Setlow and Setlow, 1962; Pan et al., 2012; San Martín, 2012). Setlow et al 1962 used this concept to investigate the role of thymine dimers in the biological damage to microbes by UV light. Other studies from that time period used this type of direct photocleavage to further investigate the prevalence thymine dimers in UV-induced damage or reported on the phenomenon using absorbance measurements (Johns et al., 1962; Setlow and Carrier, 1963; Johns et al., 1964; San Martín, 2012). Recently, Pan et al 2012 used direct photocleavage from sequential irradiations to investigate the effect of neighboring purines on CPD formation (Pan et al., 2012; San Martín, 2012). It is important to note direct photocleavage of CPDs is generally observed only through high doses of UV irradiation in intact DNA where the initial dose of 280 nm is at least 100 mJ/cm^2 (Setlow and Setlow, 1962; San Martín, 2012). The degree of photoreversal increases with increasing lower wavelength irradiation.

2.2 Motivation and Objectives

Medium-pressure (MP) UV lamps produce an emission spectrum spanning the UV range allowing for sample exposure to multiple wavelengths as opposed to low-pressure (LP) UV lamps which have a monochromatic emission at 253.7 nm. Figure 1 illustrates the polychromatic versus monochromatic emission of MP and LP lamps, respectively. For UV systems utilizing LP

UV lamps, direct photocleavage of CPDs is not a concern; however, the polychromatic emission of MP lamps allows the possibility of DNA exposure to multiple wavelengths. Therefore, there exists the opportunity for direct photocleavage of CPDs through MP UV irradiation. MP UV lamps are becoming increasingly popular, as they have been shown to exhibit increased effectiveness for the inactivation of challenge microbes such as adenovirus (Linden et al., 2007). Adenovirus displays extraordinary resistance to LP UV irradiation requiring a dose of 186 mJ/cm^2 for 4-log reduction of the virus (USEPA 2006a). MP UV irradiation has been demonstrated to achieve 4-log reduction of adenovirus at doses of 60-80 mJ/cm^2 (Linden et al., 2007). Furthermore, MP UV irradiation has been shown to limit the degree of photoreactivation seen after the UV exposure in *E. coli* (Zimmer and Slawson, 2002). Although there is convincing research for the increased efficacy of MP UV lamps compared to LP UV, there have been observations that MP UV results in slightly less DNA damage for equivalent doses (Eischeid et al., 2008). Essentially, MP UV is a completely proven effective disinfection technique; however, since there is the possibility for direct photocleavage, there exists the possibility that the technology is not completely optimized.

In this paper, the possibility of direct photocleavage of CPDs is considered in the context of MP UV disinfection processes. Specifically, the research aims to 1.) determine if direct photoreversal of UV induced DNA damage occurs in cellular DNA (previous research has used isolated DNA in the irradiations) and 2.) determine if the amount of high and low-wavelength UV-C typically present in MP UV doses can result in the direct photocleavage of CPDs. These questions are addressed using culture techniques and methods to quantify the amount of DNA damage, specifically quantitative polymerase chain reaction (qPCR). qPCR is not specific for CPDs, rather it will measure all DNA damage present in the amplified region. Therefore, it is a

good indicator of whether or not direct photocleavage of CPDs can account for enough DNA damage reversal for the DNA to retain viability. Further examining this concept with culture techniques for bacterial growth will allow for the determination of whether or not cell viability is affected by direct photoreversal of DNA damage.

2.3 Materials and Methods

2.3.1 UV Exposures and Sample Preparation

A bench-scale, collimated beam apparatus equipped with a 1-kW MP UV lamp (Calgon Carbon Corporation Inc., Pittsburgh, PA, USA) was used for the exposures. The lamp was outfitted with 280 and 228 nm bandpass filters for the wavelength specific exposures; the emission spectrums of the filters are shown in Figure 2-3. Incidence irradiance at the sample surface was measured using an IL-1700 radiometer complete with a SED 240 detector and W-diffuser (International Light, Peabody, MA, USA) with settings specific for bandpass filter emission. Exposure time for each UV dose was calculated as described in Bolton and Linden 2003. Briefly, sample absorbance was measured using a Cary 100 Spectrophotometer and used to calculate average irradiance for a continuously stirred batch system. Average irradiance was germicidally weighted using the DNA absorbance spectrum and divided by target UV dose to obtain specific exposure times. Nonhomogeneous lamp emission was accounted for using a Petri factor as a correction (Bolton and Linden, 2003).

Ampicillin/streptomycin resistant *E. coli* was grown to late log phase in Tryptic Soy Broth (TSB) containing ampicillin/streptomycin. 1 mL of the solution was washed 3 times with 1X phosphate-buffered saline (PBS) and diluted in PBS to a target concentration of 10^6 CFU/mL. Specific exposure procedure varied slightly depending on specific experimental

designs and will be discussed within design explanations.

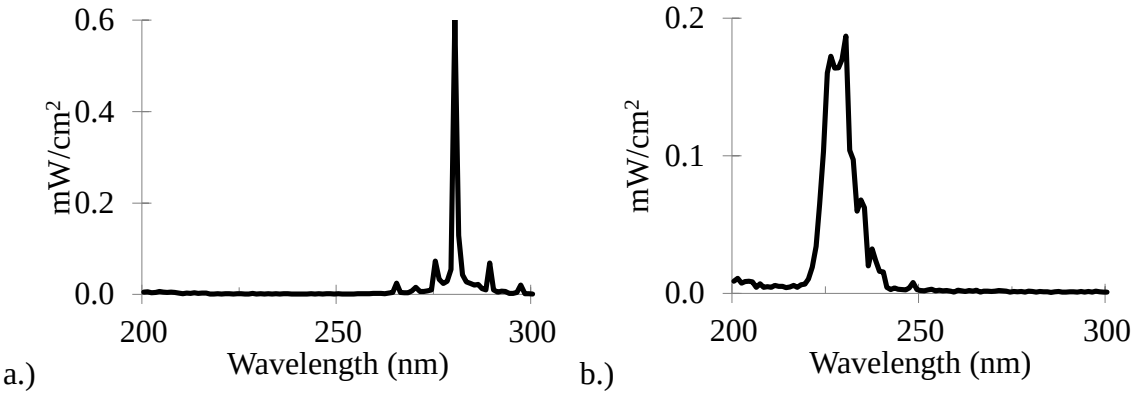

Figure 2-3: Emission spectrums of a.) 280 nm bandpass filter and b.) 228 nm bandpass filter

2.3.2 Experimental Designs

Experiments were performed using 280 and 228 nm bandpass filters. UV doses of sequential irradiations were chosen to examine a variety of initial 280 nm doses and subsequent 228 nm doses.

Design 1

Design 1 doses were designed to determine if the qPCR assay could detect photoreversal and examine the effect of the 228 nm dose on the degree of photoreversal. UV doses for Design 1 followed a general pattern of an initial dose of 120 mJ/cm^2 at either 280 nm or 228 nm; the dose design is shown in Table 2-1. For single-wavelength irradiations, the sample was exposed to an additional dose of 30, 60, 90, and 120 mJ/cm^2 of radiation at the same wavelength as the initial dose. For the multiple-wavelength irradiations, the sample was initially exposed to 280 nm (120mJ/cm^2) radiation followed by 30, 60, 90, and 120 mJ/cm^2 of 228 nm light. For each initial exposure 25 mL of sample was exposed in a 60 mm petri dish for 120 mJ/cm^2. 5 mL of the initial sample was used for subsequent irradiations and was exposed using a 30 mm petri dish. The

samples were continuously stirred using sterile magnetic stir bars throughout the entire exposure. 200 μL of sample was collected after exposure completion for DNA damage analysis. Each multiple-wavelength exposure was performed two times independently and single-wavelength control exposures were performed once.

Table 2-1: UV dose designations for Design 1

Sample	Initial 280 nm Dose (mJ/cm^2)	Subsequent 280 nm Dose (mJ/cm^2)	Subsequent 230 nm Dose (mJ/cm^2)
1	120	0	0
2	120	0	30
3	120	0	60
4	120	0	90
5	120	0	120
280 Control 1	120	0	0
280 Control 2	120	30	0
280 Control 3	120	60	0
280 Control 4	120	90	0
280 Control 5	120	120	0
230 Control 1	0	0	120
230 Control 2	0	0	150
230 Control 3	0	0	180
230 Control 4	0	0	210
230 Control 5	0	0	240

Design 2

Design 2 doses were designed to further investigate direct photoreversal by examining the effect of varying the initial 280 nm dose of the degree of photoreversal. Samples were exposed initially to 280 nm light up to 100 mJ/cm^2 in increments of 10 mJ/cm^2. Multiple-wavelength exposures were followed by 10 mJ/cm^2 of 228 nm light. The UV dose design is shown in Table 2-2. 5 mL of sample in a 30 mm petri dish was used for initial exposure. After initial exposure of 280 nm light, 200 μL was collected for analysis and the remaining sample was subsequently exposed to 10 mJ/cm^2 of 228 nm light. 200 μL was again collected for analysis following completion of the exposure. Each exposure was performed two times independently.

Table 2-2: UV dose designations for Design 2

Sample	Initial 280 nm Dose (mJ/cm^2)	230 nm Dose (mJ/cm^2)
1	10	0
2	20	0
3	30	0
4	40	0
5	50	0
6	60	0
7	70	0
8	80	0
9	90	0
10	100	0
11	10	10
12	20	10
13	30	10
14	40	10
15	50	10
16	60	10
17	70	10
18	80	10
19	90	10
20	100	10

Design 3

For Design 3, doses were designed to examine the amount of photoreversal that is possible as a result of MP UV lamp exposures. UV doses for 280 nm and 228 nm were calculated to mimic the amount of radiation in total MP doses that is attributed to the ranges 275-285 nm and 225-235 nm, respectively. The percent of the total average irradiance that 275-285 nm and 225-235 nm accounted for was determined. The percent values were then used to find the amount of the total MP dose in mJ/cm^2 these ranges accounted for. The determined dose value was the target value used in the exposure time calculations. MP doses up to 1000 mJ/cm^2 were used in increments of 100 mJ/cm^2. The UV dose design is shown in Table 2-3. The range of 275-285 nm accounted for ~10% of the total MP radiation and the range of 225-235 nm

accounted for 6-7% of the total MP radiation. The percent of total dose corresponding the wavelength ranges varied slightly (± 0.05%) for each exposure as the sample absorbance varied slightly between experiments. Collection process followed same pattern as Design 2: 200 μL collected after initial 280 nm exposure and after subsequent exposure at 228 nm. Each exposure was performed two times independently.

Table 2-3: UV dose designations for Design 3

Sample	Overall MP Dose* (mJ/cm^2)	Corresponding 280 nm Dose (mJ/cm^2)	Corresponding 230 nm Dose (mJ/cm^2)
1	100	10	0
2	200	20	0
3	300	30	0
4	400	40	0
5	500	50	0
6	600	60	0
7	700	70	0
8	800	80	0
9	900	90	0
10	1000	100	0
11	100	10	6.5
12	200	20	13.0
13	300	30	19.5
14	400	40	26.0
15	500	50	32.5
16	600	60	39.0
17	700	70	45.5
18	800	80	52.0
19	900	90	58.5
20	1000	100	65.0

*Indicates the MP UV lamp dose used to design the single- and sequential-wavelength doses

2.3.3 Colony Forming Units (CFU) Growth and Enumeration

UV doses were determined via the same method as Design 3 to mimic the amount of radiation the sample will receive from 280 nm and 228 nm in MP exposures. Briefly, 20 mL of sample in a 60 mm petri dish was initially exposed to 280 nm dose and 1 mL of the sample was

collected for analysis. The remaining sample was subsequently exposed to 228 nm light for the specified dose and 1 mL was collected upon completion. 20 mL of sample in a 60 mm petri dish was also used for single-wavelength 228 nm exposures with 1 mL of sample collected for analysis. All plating was completed the same day as the exposure with less than one hour between exposure and plating. Serial dilutions were performed immediately prior to plating.

Antibiotic-containing Tryptic Soy Agar (TSA) plates were prepared and allowed to solidfy for at least 24 hours under refrigeration before plating. Samples were diluted in sterile 1X PBS and 100 μL of sample was pipetted to surface of TSA plates and spread using an L shaped glass stick. Each sample was plated in triplicate. Plates were allowed to incubate at 37°C 18-24 hours. The volume of sample used and the dilution factor were taken into account when determining CFU counts. Log inactivation was calculated as $\log(N_0/N)$ where N is CFU/mL for the sample and N_0 is CFU/mL for the untreated control.

2.3.4 Real-time quantitative polymerase chain reaction (qPCR)

DNA was extracted using DNeasy Blood and Tissue Kit (Qiagen, Valencia, CA). Primers and probe for the E. Coli 16S rDNA gene were developed as described in Rudi et al 2010 and the designs are shown in Table 2-4. Fragment size was 1504 base pairs. Primers and probe synthesized by International DNA Technologies. Each sample was prepared 7.5 μM of forward and reverse primer, PrimeTime probe, nuclease-free water, master mix (Promega, Madison, WI) consisting of 2 units of GoTaq polymerase, 1 X of GoTaq Buffer, and 2 μL of DNA solution for a total volume of 25 mL. qPCR samples were performed in duplicate using a MJ MiniOpticon™ Real-Time PCR machine (Bio-Rad, Hercules, CA). The thermocycle for the PCR assay is shown in Table 2-5.

Table 2-4: Primer and probe information (sequences designed by Rudi et al., 2010)

Primer	Sequence	Genome Region*	Fragment Size (bp)
Forward Primer	AAGAGTTTGATCATGGCTCA	42	1504
Reverse Primer	CGGTTACCTTGTTACGACTT	1546	
Probe	TATCGCGGCTGCTGGCAC		

*Position relative to *E. coli* 16S rRNA with respect to 5' end

Table 2-5: qPCR thermocycle

Step	Temp (°C)	Time (s)
Denaturation	90	30
Annealing	55	30
Synthesis	72	90

2.3.5 Statistical Analysis

DNA quantification was determined using a 10-fold dilution curve. A standard curve was developed from the dilutions and number of gene copies in log-scale was calculated from the number of PCR cycles required for a specific fluorescence signal. Log reduction in DNA was calculated as $\log(N_0/N)$, where N is amount of amplifiable DNA in the sample and N_0 is the amount of DNA in untreated control. Quantification analyses and calculations were carried out in Excel. Statistical analyses including ANOVAs and confidence intervals were carried out using MiniTab. Averages of trials are reported in graphs, but regressions were carried out using all samples.

2.4 Results and Discussion

2.4.1 Plate Count Results

As described previously in the text, the spread-plating technique was used to determine the CFU of *E. coli* exposed to sequential 280 and 228 nm irradiation and single-wavelength

exposures at 280 nm and 228 nm. Doses for the exposures were calculated from the amount of irradiation that can be attributed to the ranges 275-285 nm and 225-235 nm in typical MP UV lamp emission for the 280 nm and 228 nm band pass filters, respectively. The results are reported as overall MP doses represented by the filtered irradiations. Log inactivation values for single-wavelength and multiple-wavelength exposures representative of the amount of radiation attributed to MP doses 50, 100, and 150 mJ/cm^2 are presented in Figure 2-4. Single-wavelength exposure at 280 nm and 228 nm yielded the expected result of increasing *E. coli* inactivation with increasing dose. Multiple-wavelength exposure of 280 nm followed by 228 nm produced greater inactivation of *E. coli* than either single-wavelength exposure for the same representative MP doses with almost complete inactivation resulting from MP doses of 100 and 150 mJ/cm^2. The multiple-wavelength response seemed to follow the same trend as that of the 280 nm response.

Using the culture techniques, there was no indication that exposing *E. coli* to a 228 nm radiation reversed UV-induced damage from 280 nm exposure. Instead, multiple-wavelength irradiations seem to have an additive effect and result in a greater level of inactivation than single-wavelength exposures. Figure 2-4 also shows the sum of the single-wavelength log reduction values and the results indicate that the sum of the values is almost identical for the 100 mJ/cm^2 irradiations. UV light is known to cause damage to cellular macromolecules other than DNA such as proteins (Eischeid and Linden, 2011). The increased dose, especially at low-wavelengths, most likely increased the amount of damage to other cellular components leading to a greater amount of inactivation. Furthermore, *E. coli* is very sensitive to UV radiation, usually only requiring 5-10 mJ/cm^2 for 4-log reduction (Wright et al. 2000). Successful inactivation of *E. coli* can take place as very few lesions formed in the DNA can disrupt the

reproductive and transcriptional machinery (Oguma et al., 2002; Eischeid and Linden, 2007). Therefore, even if minor reversal of CPDs did take place, it would most likely not provide sufficient repair of the damage to return cell viability. The extreme sensitivity of *E. coli* and the probable increased damage to proteins likely prevented observation of DNA damage reversal from multiple-wavelength exposures when examined using CFU counts.

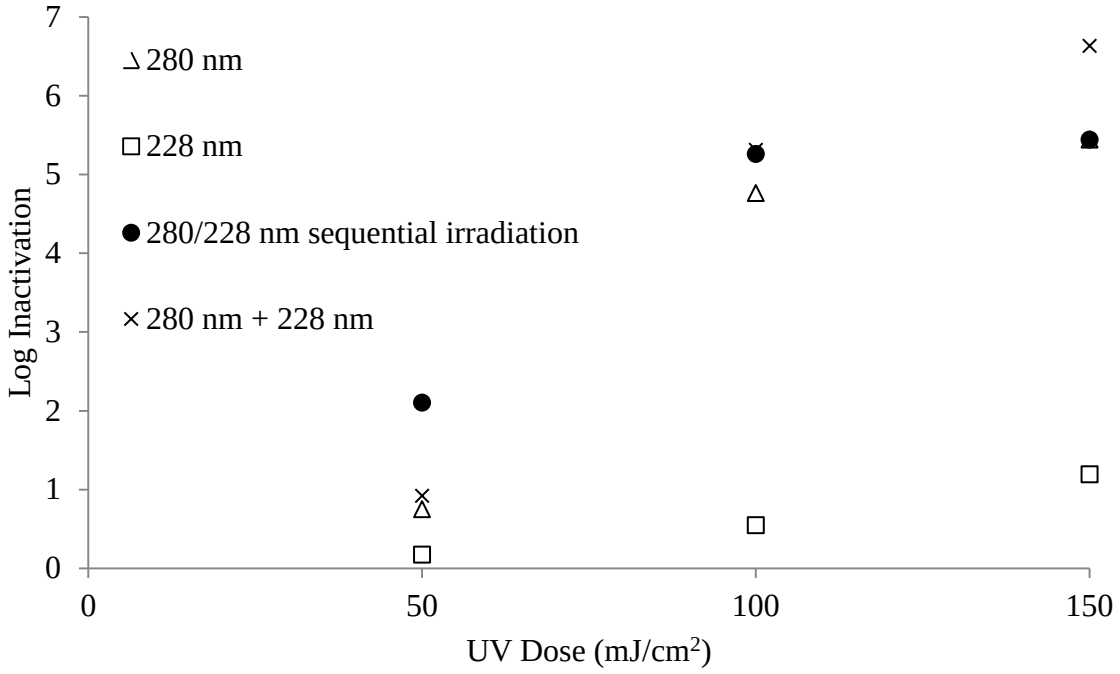

Figure 2-4: Log inactivation values measured by CFU counts for single-wavelength and sequential-wavelength irradiations. X-axis shows the representative MP doses from which the wavelength-specific doses were determined. The y-axis is the log inactivation.

2.4.2 PCR Assays

Design 1

Figure 2-5 shows the results of multiple-wavelength irradiations and the single-wavelength control irradiations. For each exposure, the sample was exposed to an initial dose of 120 mJ/cm^2 at either 280 nm or 228 nm followed by subsequent exposures of 30, 60, 90, and 120 mJ/cm^2 at the specified wavelength. For the 280 nm and 228 nm single-wavelength exposures,

amplifiable DNA decreases with increasing dose for both wavelengths. 280 nm irradiation demonstrated greater DNA damage after 120 mJ/cm^2 than an equivalent dose at 228 nm. For multiple-wavelength exposures, 280 nm + 228 nm irradiation resulted in increased amplifiable DNA following an initial 120 mJ/cm^2 dose of 280 nm irradiation. A dose of 120 mJ/cm^2 of 228 nm light provided a log reduction in amplifiable DNA of 3.34 compared the sample's initial log reduction of 4.97 resulting from the exposure only to 120 mJ/cm^2 of 280 nm light.

PCR results obtained from Design 1 exposures clearly demonstrated DNA damage reversal in samples exposed sequentially to irradiation from 280 nm followed by 228 nm. There was a significant decrease in the log reduction of amplifiable DNA observed from the initial dose 120 mJ/cm^2 at 280 nm with each increased dose of 228 nm light. Linear regression for multiple-wavelength irradiations showed a negative slope of -0.014 between log reduction and increasing 228 nm exposure (p-value of slope: <0.001). This result indicates that exposure to 228 nm resulted in DNA repair as indicated by the increase in the amount of amplifiable DNA in samples that were previously exposed to 280 nm. An increased amount of amplifiable DNA suggests there are less lesions blocking amplification during the PCR process. Positive linear relationships were observed for 280 nm (slope = 0.008 and p-value = 0.099) and 228 nm (slope = 0.007 and p-value = 0.002) single-wavelength exposures. This implies the single-wavelength exposures result in the formation of more amplification blocking lesions and further suggests the increase in amplifiable DNA seen in coupled-wavelength exposures are a direct result of 228 nm light.

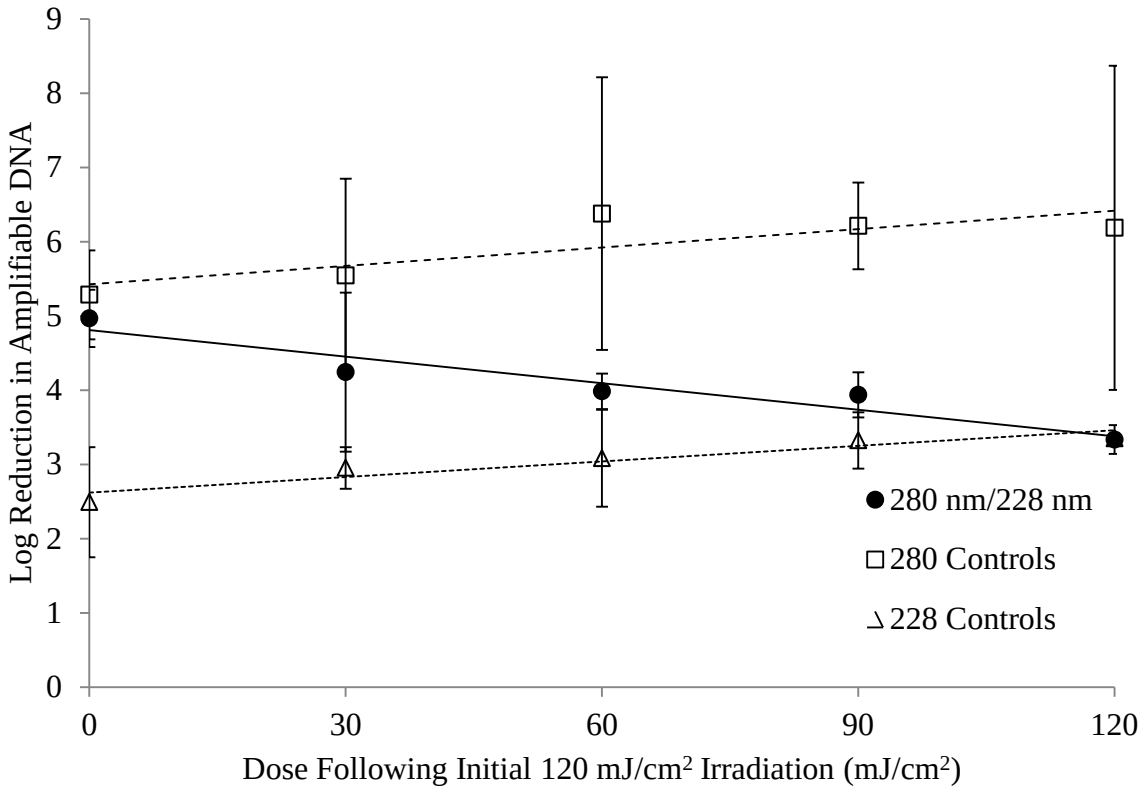

Figure 2-5: Log reduction of amplifiable DNA extracted from E. coli at various dosing conditions. The x-axis shows the subsequent dose of UV light applied after an initial dose of 120 mJ/cm^2 at the specific wavelength. The y-axis is the log reduction values for amplifiable DNA. Error bars are shown to demonstrate 80% confidence intervals. Closed circle: sample initially exposed to 120 mJ/cm^2 at 280 nm followed by doses of 228 nm shown on x-axis. Open square: samples were initially exposed to 120 mJ/cm^2 at 280 nm followed by 280 nm doses shown on x-axis. Open triangle: samples were initially exposed to 120 mJ/cm^2 at 228 nm followed by more 228 nm light at the doses shown on the x-axis.

The PCR assay measures not only DNA damage in the form of CPDs but also any other DNA damage inhibiting the amplification process including other photoproducts or single-strand breaks (Rodríguez et al., 2013). In addition, the major UV-induced lesion in DNA is the CPD and accounts for roughly 75% of UV-induced lesions in the DNA (Sinha and Häder, 2002). Direct photocleavage of CPDs occurs at high efficiency leading to the assumption the majority of CPDs can be reversed given enough low-wavelength light (Pan et al. 2012). As shown by the results, there was still a significant amount of DNA damage present after 120 mJ/cm^2 of sequentially applied 228 nm light. This can be attributed to non-CPD UV-induced damage present from initial 280 nm exposure, residual CPD presence left unaffected by subsequent

exposure, and the possible induction of further UV damage caused by the secondary 228 nm exposure. Nevertheless, the trend of increased amplifiable DNA with increasing 228 nm irradiation signifies the direct photoreversal of some of 280 nm induced DNA damage. Furthermore, the absolute value of the negative slope of the coupled wavelength radiation is close to 2X greater than the slopes of the single wavelength exposures. This suggests CPD reversal is occurring at a greater rate than new damage formation after an initial damage induction by 120 mJ/cm^2 of 280 nm UV light. The amount of DNA damage reversal observed also takes into account the possible formation of new damage; therefore, it is plausible to assume the amount of CPD reversal is actually greater than what appears in the PCR results.

Design 2

Figure 2-6 presents the results from Design 2 in which the initial dose of 280 nm irradiation was varied and the samples were subsequently exposed to 10 mJ/cm^2 of 228 nm irradiation. 280 nm irradiation alone showed a positive trend in DNA damage as dose increased, as expected. When followed by 10 mJ/cm^2 of 228 nm irradiation, the degree of DNA damage followed a similar trend to the single 280 nm dose response of amplifiable DNA. Both data sets follow a positive linear relationship with increasing DNA damage as initial 280 nm dose increases. There are slight deviations between the sequential and single-wavelength data points after an initial 280 nm of 50 mJ/cm^2; however, as seen on the graph, the 80% confidence intervals clearly overlap at all levels. Therefore, this deviation can't be considered significantly different. The 10 mJ/cm^2 is a relatively small amount of subsequent 228 nm irradiation compared to the doses used in Design 1 which showed significant increases in amplifiable DNA with subsequent 228 nm irradiation up to 120 mJ/cm^2. Once again, direct DNA damage reversal, or direct photocleavage, is thought to only occur with CPDs and the PCR assay will account for all

DNA damage including 6-4 photoproducts and less frequent damage such as single-strand breaks. Since 10 mJ/cm^2 only provides slight capability for direct photocleavage and the PCR assay exhibits sensitivity to all UV-induced DNA damage, minor CPD reversal would most likely not make a significant change in the PCR results. Nonetheless, this design still helps to provide insight into the sensitivity of the PCR assay and its ability to detect DNA damage reversal. It shows that it is not sensitive enough to detect minor CPD cleavage.

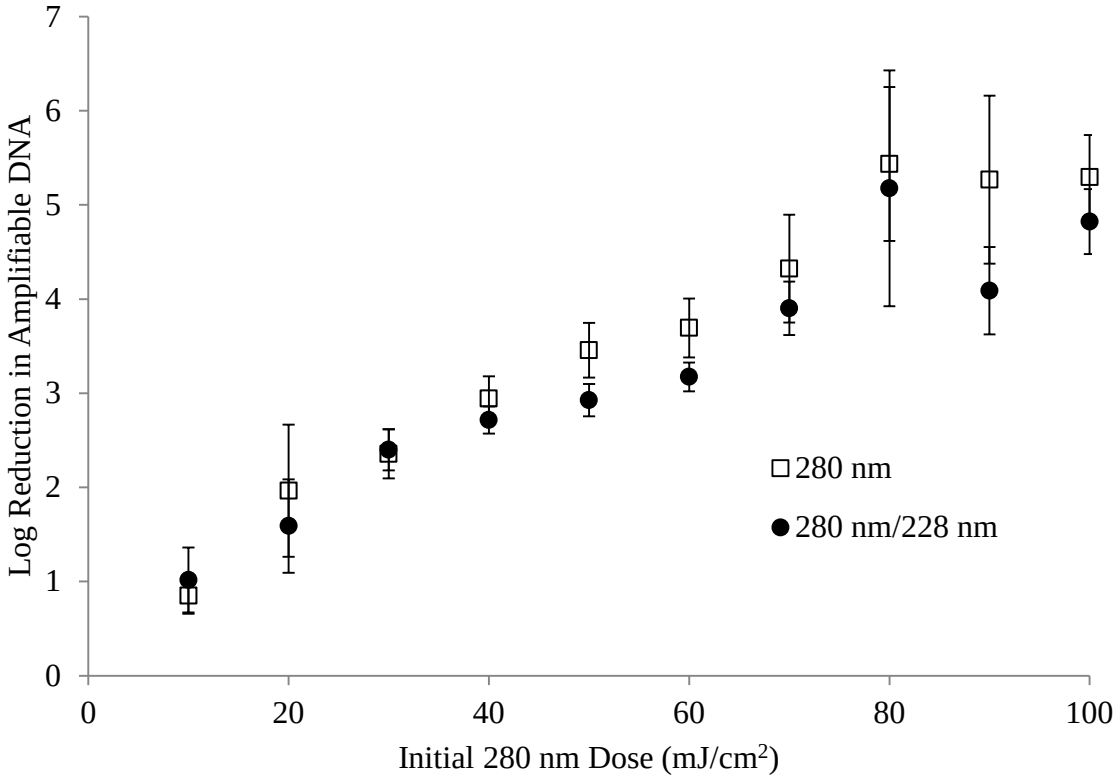

Figure 2-6: Results of single-wavelength doses of 280 nm and subsequent irradiations of 10 mJ/cm^2 at 228 nm. The x-axis shows the total or initial dose of 280 nm. Coupled-wavelength samples are followed by 10 mJ/cm^2 of 228 nm light. Error bars represent 80% confidence intervals. Open square: sample exposed to only 280 nm light at doses shown on x-axis. Closed circle: samples exposed to 280 nm light at doses shown on x-axis followed by 10 mJ/cm^2 of 228 nm light.

Design 3

Design 3 used 280 nm and 228 nm doses calculated from the amount of radiation that can

be attributed to wavelength ranges 275-285 nm and 225-235 nm in typical MP doses, respectively. The PCR assay results are shown in Figure 2-7. For the single 280 nm exposure, the trend in DNA damage demonstrated a positive linear relationship between increasing dose and a decrease in amplifiable DNA, as indicated by increasing log reduction values. However, as seen on the graph, the sequential-wavelength irradiation data shows a different trend than the single-wavelength irradiations resulting in less log reduction of amplifiable DNA, indicating less DNA damage present. The degree of DNA damage reversal increases with MP dose; however, the difference between the single and sequential-wavelength log reduction values is only significant after a MP dose of 600 mJ/cm^2 as indicated by the 80% confidence intervals.

DNA damage during the sequential-wavelength irradiations is increasing with MP dose, meaning that a representative dose of 900 mJ/cm^2 results in more DNA damage than a dose of 800 mJ/cm^2. This can be a result of the increased damage of the higher initial 280 nm dose or the induction of further UV-induced DNA damage resulting from 228 nm irradiation. However, the significance of the data set lies in the observation that subjecting the samples to 228 nm light will increase the amount of amplifiable DNA compared to samples exposed solely to 280 nm light, which suggests there are fewer UV-induced lesions present in the DNA of *E. coli* exposed to multiple wavelengths. A MP dose of 1000 mJ/cm^2 for the sequential-wavelength exposure demonstrated comparable DNA damage as a MP dose of 600 mJ/cm^2 for a 280 nm single-wavelength exposure.

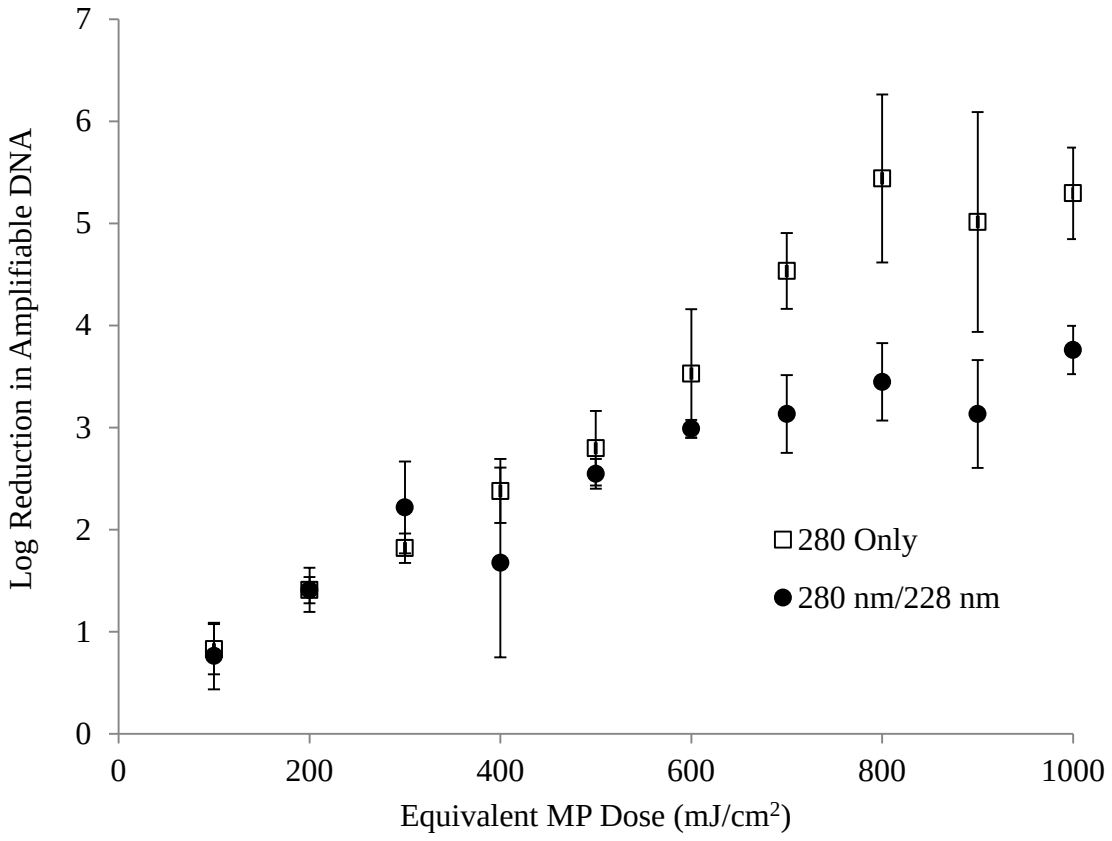

Figure 2-7: Results of single and sequential-wavelength irradiations relevant to MP doses. X-axis shows the representative MP doses from which the wavelength-specific doses were determined. The y-axis is the log reduction in amplifiable DNA. The error bars represent an 80% confidence interval. Open square: samples were only exposed to designated dose at 280 nm. Closed circle: samples were initially exposed to designated dose at 280 nm followed by designated dose at 228 nm.

Figure 2-8 shows the difference in amplifiable DNA between single and coupled-wavelength exposures. This was calculated by subtracting log reduction of 280 + 228 nm exposures from 280 nm exposures and is representative of the amount of damage reversal. The amount of damage reversal increases as the amount of damage from the initial UV dose increases. The presence of 228 nm light therefore reduces the damaging effects of UV at higher wavelengths for high doses of UV light.

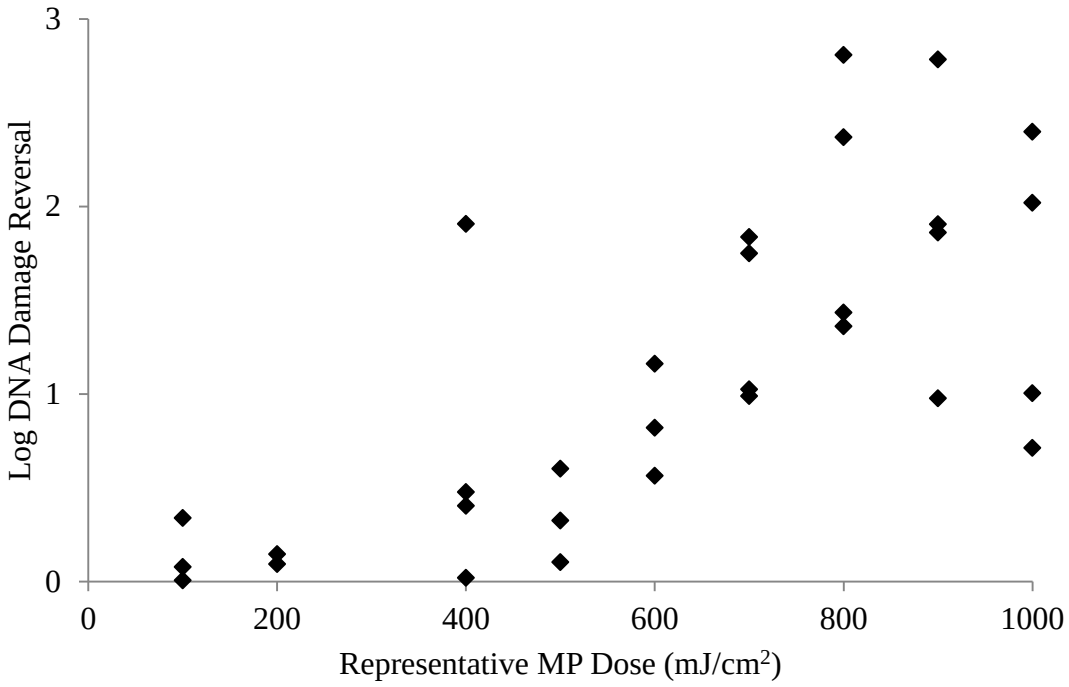

Figure 2-8: Calculated amount of DNA damage repair resulting from 230 nm light. X-axis shows the representative MP doses from which the wavelength-specific doses were determined.

2.4.3 Impact of CPD Reversal

PCR results suggested CPD reversal can occur through sequential irradiations in intact, cellular DNA. However, significant reversal only occurred after high initial irradiations of 280 nm and high doses of subsequent 228 nm light exposure. For instance, a representative MP dose of 600 mJ/cm^2 is required for any detection of significant CPD reversal by the PCR assay. We speculate that these doses are necessary in order to observe DNA damage reversal because a higher dose increases the amount of CPDs present in the DNA. Basically, increasing the concentration of CPDs in the DNA will increase the possibility of that lower wavelength light will hit and directly cleave a CPD. Similarly, increasing the amount of lower wavelength irradiation increases the likelihood that the light will come into contact with the CPD and effectively cleave the dimer CPDs resulting from lower doses of UV light could be effectively cleaved with exposure to low wavelength UV-C light, but the possibility of specific CPD

absorption by such UV-C light is unlikely with low CPD concentration. High doses simply increase the probability of CPD photocleavage by increasing CPD concentrations and increasing low-wavelength UV-C light.

There are several factors that must be considered when attempting to apply these results to typical MP irradiation processes. Typical MP UV doses required for disinfection purposes are at 50-250 mJ/cm^2. At these doses, results suggest direct CPD photocleavage will most likely not significantly affect the successful inactivation of microbes. However, studies have indicated that relatively small amounts of CPDs need to be present in *E. coli* in order to produce effective inactivation (Oguma et al., 2002; Eischeid and Linden, 2007). Given the sensitivity of some microbes to CPDs, there exists the possibility that direct CPD photocleavage could return viability to the individual organism through the cleavage of 1-2 CPD lesions. However, the results indicate that when dealing with large numbers of microbes and seeking 4-log inactivation, the doses would have to be exceedingly high for direct CPD photocleavage to influence disinfection practices and UV doses. Furthermore, MP UV irradiation provides polychromatic emission resulting in microbial exposure to more than just 280 nm and 228 nm light, which also induces significant damage to DNA and other cellular macromolecules (Eischeid and Linden, 2011). This is supported by the CFU counts which showed an additive effect on inactivation for multiple-wavelength exposures. Another aspect of MP UV irradiation is that it does not have sequential wavelength exposure. Microbes are exposed to the entire polychromatic emission at once. It is difficult to speculate how this could effect CPD reversal.

2.5 Conclusions

The PCR results of sequential wavelength irradiations indicate direct DNA damage reversal occurs using high doses of 280 nm and 228 nm light. This DNA damage reversal is most

likely the direct photocleavage of CPDs. However, the results suggest that direct photoreversal of UV-induced DNA damage will have little effect on MP UV irradiation for disinfection purposes. The high doses required for significant damage reversal greatly exceed those used in practical MP applications. Further, the non-sequential nature and increased UV-induced damage to other cellular components of MP emission decreases the likelihood that CPD photoreversal could reverse MP UV-induced damage.

Although CPD photocleavage does not appear to seriously affect MP-UV-induced DNA damage, it is still interesting to examine direct photoreversal of DNA damage in with respect to engineering applications. This research investigated direct photoreversal using genomic DNA intact in viable cells as opposed to other studies, which utilized isolated DNA. The results indicated direct photocleavage of CPDs is possible after sufficient concentrations of the lesion have been formed in cellular DNA. However, this research brings up the questions of whether and to what degree direct photocleavage of CPDs could take place when CPDs are formed via other wavelengths such as 250-260 nm, which accounts for the majority of DNA damage induction from MP UV lamps. Future research could attempt to increase sensitivity of CPD detection and quantification to determine the degree, if any, of direct photoreversal at lower doses.

3. Adenoviral MP UV Inactivation: Data Compilation and Analysis and Wavelength-Specific Protein Damage

3.1 Introduction

Adenovirus poses a significant challenge to UV disinfection processes and their ability to

provide clean, safe drinking water. Adenovirus exhibits significantly greater resistance to UV irradiation than all other viral pathogens (Linden et al., 2007; Rodríguez et al., 2013). High doses of UV irradiation are required to achieve adequate reduction of the virus, making adenoviral reduction the limiting factor in viral UV reactor validation and numerous regulations including the Long Term 2 Enhanced Surface Water Treatment Rule (LT2ESWTR) and the Groundwater Rule, which states UV disinfection alone is not sufficient for groundwater treatment (Eischeid et al., 2011; USEPA, 2006b; USEPA, 2006c). Adenovirus is pathogenic, can cause a variety of serious diseases, and can even result in death in rare cases (Yates et al., 2006; Eischeid et al., 2011). The extreme UV resistance and pathogenicity of adenovirus has made the virus the focus a considerable amount of research concerning its prevalence, pathogenicity, composition, and mechanism of resistance. Recently, research has shown a dramatic difference in the resistance of adenovirus to MP versus LP irradiation demonstrating the virus is significantly more susceptible to MP irradiation (Linden et al., 2007; Shin et al., 2009; Guo et al., 2010). This has been an exciting discovery for the UV industry as it helps to alleviate the challenge posed by the virus to UV disinfection by greatly decreasing the required doses for UV reactor validation. However, the findings bring up questions concerning regulations and the largely unknown reason for increased susceptibility of adenovirus to MP irradiations. Furthermore, increased use and advancement of MP lamps has fostered issues concerning the low-wavelength emission, as explained earlier in the text, of MP lamps, which will be discussed later in the chapter. The above concepts are the motivation for this research. Essentially, this research aims to investigate the differences in adenoviral susceptibility to MP and LP irradiation and the reasons behind the difference. This was accomplished through analysis of past research concerning the topic and the examination of adenoviral protein damage as a result of specific wavelengths throughout the

UV-C spectrum.

3.1.1 Adenovirus Structure and Infection

Adenoviridae comprises a family of viruses infecting a wide-variety of species. Within this family, there are 52 serotypes of adenoviruses known to infect humans which can cause a variety of infections and diseases (Yates et al., 2006; Eischeid and Linden, 2011). Adenoviruses are non-enveloped and are icosahedral particles. Their genomes consist of double-stranded DNA (dsDNA) ranging from around 30-40 kb in length depending on the serotypes (Eischeid et al., 2011). The general structure consists of a protein capsid surrounding a viral core comprised of both the dsDNA genome and proteins. There are 11-15 viral proteins, some of which will be briefly discussed here (Greber et al., 1993; Eischeid et al., 2011).

Hexon

The hexon protein accounts for the majority of the viral capsid. Hexon protein structure is arranged in a highly folded design which results in capsid stability. The function of the hexon protein has been considered to be predominantly architectural; however, recent findings suggest the protein does play a role in the adenovirus-host interaction along with bind and entry into the host. The hexon protein has a molecular weight of 108 kD (Eischeid, 2009; San Martín, 2012)

Fiber Protein

The fiber protein, also known as polypeptide IV, is responsible for the attachment of the virus to the host cell. The target host receptor for the fiber protein is the coxsackie and adenovirus receptor (CAR) on the cell surface. The flexibility of the fiber protein is a noteworthy factor as sufficient bending by the fiber protein is required in order for subsequent steps in the infection. The fiber protein has a molecular weight of 62 kD (Eischeid, 2009; San Martín, 2012).

Penton Base

The penton base protein, also known as polypeptide III, is involved in the initial stages of infection along with the fiber protein. After the fiber protein attachment, the penton base binds to host cell ligands, known as integrins, and result in endocytosis or internalization of the virus. Internalization is thought to spur the disassembly of the virus capsid. The penton base protein has a molecular weight of 85 kD (Eischeid, 2009;San Martín, 2012).

Polypeptide IIIa

Polypeptide IIIa is a protein which has been suggested to play a role in the successful assembly and release of the virion from the host cell. It has also been postulated to play a role in signaling the release of the genome. Polypeptide IIIa has a molecular weight of 63.5 kD (Eischeid, 2009; San Martín, 2012).

Polypeptide VI

The action of polypeptide VI is dynamic and present throughout the infection cycle. It is responsible for host membrane disruption after the attachment and capsid disassembly for successful entry into the cytoplasm and VI aids in transport to the host nucleus. Polypeptide VI has a very important function in mediating activation of transcription of the adenoviral genome leading to gene expression. Further, it heavily assists with the particle assembly process. Polypeptide VI has a molecular weight of 22 kD (Eischeid, 2009; San Martín, 2012; Schreiner et al., 2012).

Polypeptide VIII

The role of polypeptide VIII is not as well characterized as the other proteins present in the infectious stage. Its function is considered to be mostly architectural as it associates with the

hexon and possibly involved successful genome packaging. It has been implicated to help resist heat damage. Polypeptide VIII has a molecular weight of 7.6 or 12.1 kD (Eischeid, 2009; San Martín, 2012).

Polypeptide IX

Polypeptide IX is present on the outside of the capsid and encompasses the entire virion generally. The protein is highly flexible and it is considered to be a type of net to keep the hexon proteins correctly arranged. Polypeptide IX has a molecular weight of 14.4 kD (Eischeid, 2009;San Martín, 2012).

Major Core Protein

The major core protein is the dominant core protein is closely associated with adenoviral DNA and forms a nucleosome with the DNA. The major core protein is abundant with positively-charged amino acids in order to couple with the backbone of viral DNA which is negatively charged. The major core protein has a molecular weight of 18.5 kD (Eischeid, 2009).

Minor Core Protein

The minor core protein forms a shell around the nucleosome and is also rich with positively-charged amino acids to enable association with the viral DNA backbone. The minor core protein has a molecular weight of 41.6 kD (Eischeid, 2009).

Protease

Adenovirus also contains a protease enzyme in its core which is responsible for cleaving various protein precursors and has a molecular weight of 23 kD (Eischeid, 2009).

Terminal Protein

The adenoviral core holds a terminal protein which is involved in the DNA replication

process. The terminal protein has a molecular weight of 55 kD (Eischeid, 2009).

The proteins described above are the major proteins present in the mature adenovirus when the virion is capable of infection. There are other proteins present during replication and assembly in the host cell; however, UV light will most likely only affect proteins present in mature viruses so these are the ones considered most important. Also, it has been implicated that specific protein structure and function can vary slightly with serotype, but the above descriptions were aimed to give a general overview and insight into the functions and structure of typical adenovirus particles.

3.1.2 Infection

Much of the infection process of adenovirus can be pieced together by the above descriptions of the proteins; however, this section will briefly outline the general process from attachment to release. Adenovirus infects cells similarly to other non-enveloped viruses. The virion attaches to the host cell via fiber protein attachment to host cell surface protein CAR (Bewley, 1999; Eischeid et al., 2011). Upon attachment, penton base proteins induce internalization of the virion into the cell which also stimulates disassembly of the viral capsid. The viral genome and some associated proteins are transferred to the cytoplasm and transported to the cell nucleus. The virus utilizes host machinery to replicate its own DNA and aid in the assembly of the new viral particles. The capsid is assembled first followed by the implantation of the viral DNA and associated proteins. Fully assembled virions are then released from the cell (Bewley, 1999; Eischeid et al., 2011; San Martín, 2012).

3.1.3 Adenoviral Pathogenicity and Prevalence

Adenoviruses can cause a variety of symptoms in humans. They can be transmitted via the fecal-oral or respiratory route and can cause severe dysentery, respiratory infections, eye

infections, or urinary tract infections. Adenoviral infections are often acute in their onset and can cause asymptomatic, self-limiting, severe, or even fatal outcomes. Individuals with adenoviral infections can shed the virus for up to several years, especially in asymptomatic cases or infections in healthy adults when the individual may not be aware of the infection. This trait poses a problem even though the initial infections are not deemed severe as it can lead to increased exposure to the virus throughout populations. Those typically at risk for more severe adenoviral infections are the immunocompromised, infants, and young children. For infection affecting the immunocompromised population, the fatality rate can reach as high as 50%. Furthermore, adenovirus is a leading cause of gastroenteritis in children and has been implicated in respiratory infection epidemics in living populations in close quarters such as military barracks or boarding schools. Although adenoviral infections are typically self-limiting in healthy adults, the virus still poses a significant threat to certain populations and even the healthy as shown by some studies and recent severe cases of pneumonia (Yates et al., 2006; Eischeid et al., 2011; USEPA, 2006a).

Human adenoviruses are classified by their GC content and attachment capabilities and are grouped into six groups (A-F). There are over 50 different serotypes of human adenoviruses that can result in infection. Certain serotypes are considered endemic to circulation throughout communities and can have seroprevelance rates as high as 95%. These include serotypes 2 and 5, which showed antibody detection in 40-60% of children (Yates et al., 2006). Although most of the endemic serotypes are not as virulent as some, their prevalence throughout populations make them a definite public health hazard. Group F holds serotypes 40 and 41 which are considered to be enteric adenoviruses (fecal-oral route) as they can result in severe diarrhea causing as much as 20% of diarrhea-related hospitalizations in the developed world and are a leading cause, second

only to rotavirus, of infant mortality in developing nations. Incidences have also determined the causative agent of adenoviral diarrhea as serotypes other than 40 or 41 (Yates et al., 2006; Eischeid et al., 2011).

There still remain general questions concerning the prevalence of adenovirus in water sources, the capability for infection through waterborne, or capable of transmission via water as a transport mode, viruses in the drinking water, and the differences between serotypes in these cases. Adenovirus has been identified in both raw sewage throughout the world and some treated wastewaters (Crabtree et al., 1997). Furthermore, it can remain infective for extended periods time in water. Although no waterborne outbreaks have been linked to enteric adenoviruses, it is proven that the virus can spread via ingestion or exposure to contaminated waters and it has been detected to polluted waters (Yates et al., 2006; USEPA, 2006a). Adenovirus has also been implicated in several outbreaks at swimming pools or ponds, but such outbreaks have resulted in conjunctivitis symptoms (Crabtree et al., 1997).

3.2 Adenovirus and UV Disinfection

Viral disinfection has always been a challenge to UV-based treatment as it is typical for viruses to exhibit variable sensitivities to UV radiation. There are a number of factors implicated in this variability inlcuding the size of the virion, the composition of the genome, and the size of the genome (Eischeid, 2009). In addition, adenoviruses have the ability to utilize host machinery to repair UV-induced damage, so host cell characteristics can play an important role as well (Battigelli et al., 1993; Shin et al., 2005).

Adenovirus is considered to be the most resistant pathogen to UV irradiation. It demonstrates an astonishing resistance to LP UV irradiation compared to other pathogens (including viruses, bacteria, and protozoans). The pathogenic capability, persistence and

detection of adenovirus in water sources, and the extreme resistance to UV has made it the limiting factor for UV validation. The Ultraviolet Disinfection Guidance Manual (UVDGM) finalized in 2006 recommended adenovirus requires a LP UV dose of 186 mJ/cm^2 for 4-log reduction of the virus based on statistical analysis of published data. This recommendation was adopted by the US EPA's Long-Term 2 Enhanced Surface Water Rule (LT2ESW) as the required dose for UV disinfection of surface waters. This is a costly and difficult dose to achieve and remains a challenge for many UV disinfection users. The reason for the extreme resistance to LP UV irradiation adenovirus demonstrates has yet to come to a conclusive decision; however, it is considered that the virus itself is not resistant to LP UV, but it has a unique ability to effectively use host cell machinery to repair the induced damage.

The effect of adenovirus on the UV industry has led to a significant amount of research on the virus, especially concerning LP UV inactivation. However, recent research has demonstrated that MP UV irradiation results in a drastically increased efficiency for adenoviral inactivation. Such observations are exciting to the UV industry as they could aid in alleviating the obstacles concerning high dosing requirements for adenovirus inactivation. Recent reports indicate that a dose of 40-80 mJ/cm^2 can achieve 4-log inactivation of adenovirus (Linden et al., 2007; 2009; Shin et al., 2009; Guo et al., 2010; Eischeid and Linden, 2011; Rodriguez et., 2013). There still exists extensive variability in the data and the mechanism responsible for the increased inactivation efficiency remains unknown. Because the variability of inactivation will likely affect dose requirements for validation and there exists no extensive compilation or statistical analysis relevant data, this research aimed to compile the published data and analyze it compared to required LP UV doses.

To date, MP UV adenovirus inactivation has been the focus of far fewer studies than LP

UV. Table 3-1 is showing the publications used in the MP data compilation figures and analysis. The table shows research group and publication date, serotype used, and how inactivation was measured.

Table 3-1: Overview of published data concerning MP UV adenovirus inactivation used in analysis.

Reference	Peer Reviewed	Organism	Type	Assay	First Order Inactivation Coefficent	Experiment Type	Water Quality
Guo 2010	Yes	Adenovirus	5	Cell Culture (HEK293)	0.044	Batch	Lab
Guo 2010	Yes	Adenovirus	5	Cell Culture (PLC/PRF5)	0.046	Batch	Lab
Guo 2010	Yes	Adenovirus	5	Cell Culture (XP17BE)	0.110	Batch	Lab
Guo 2010	Yes	Adenovirus	40	Cell Culture (HEK293)	0.060	Batch	Lab
Guo 2010	Yes	Adenovirus	40	Cell Culture (PLC/PRF5)	0.061	Batch	Lab
Guo 2010	Yes	Adenovirus	41	Cell Culture (HEK293)	0.051	Batch	Lab
Guo 2010	Yes	Adenovirus	41	Cell Culture (PLC/PRF5)	0.056	Batch	Lab
Guo 2010	Yes	Adenovirus	41	Cell Culture (XP17BE)	0.094	Batch	Lab
Eischeid 2009	Yes	Adenovirus	2	Cell Culture (A549)	0.063	Batch	Lab
Linden 2009	Yes	Adenovirus	2	Cell Culture (A549)	0.166	Batch	Lab
Shin 2009	Yes	Adenovirus	2	Cell Culture (A549)	0.054	Batch	Lab
Linden 2007	Yes	Adenovirus	40	Cell Culture (PLC/PRF5)	0.100	Batch	Lab
Linden 2007	Yes	Adenovirus	2	Cell Culture (A549)	0.093	Batch	Lab
Linden 2011	Yes	Adenovirus	4	Not Stated	0.052	Batch	Phoenix WW Treatment Plant
Rodriguez 2013	Yes	Adenovirus	2	Cell Culture (A549)	0.032	Batch	Lab

Figure 3-1 shows the compilation of MP data points from the above studies and fits a general, linear regression line to the data. The data is compared to a representation of LP UV dose

requirements corresponding to 186 mJ/cm^2 for 4-log reduction of the virus.

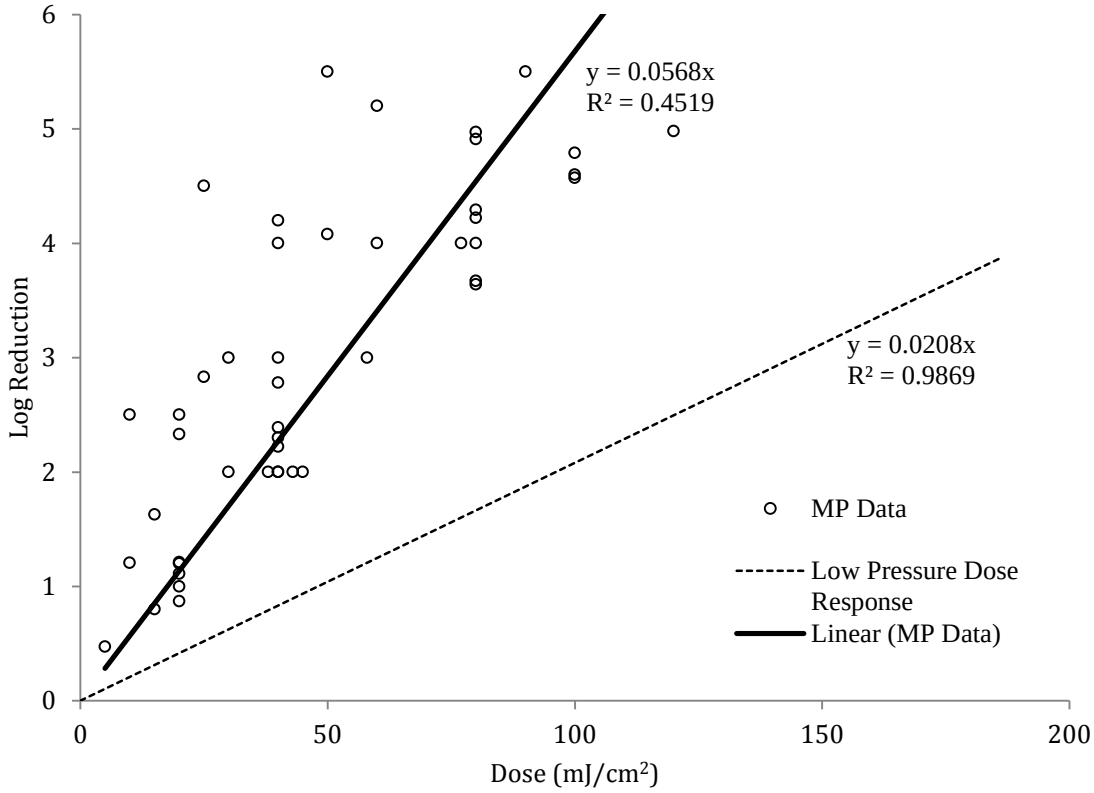

Figure 3-1: Compilation of MP UV adenovirus inactivation data with linear regression line compared to requirements for LP UV dosing

The above figure showing the compilation of MP UV log inactivation data points highlights how effective MP UV irradiation is compared to LP UV irradiation. All MP UV inactivation data points are much higher for similar doses compared to the LP UV dose requirement line. However, the LP UV dose requirement line was a conservative estimate by the Ultraviolet Disinfection Guidance Manual (UVDGM) authors based on statistical analysis of published LP UV data and a series of credible intervals. Using this compilation of MP UV data points, similar statistical analysis was performed in order to gain insight into possible assumptions that could be made for dose requirements. Figure 3-2 shows the data compilation and linear regression line along with a series of prediction intervals. Prediction intervals are used

as a credible representation of where the next inactivation data point will land given a UV dose based on a confidence level, as opposed to confidence intervals which represent the interval of where the true mean of the data will lie based on a confidence level.

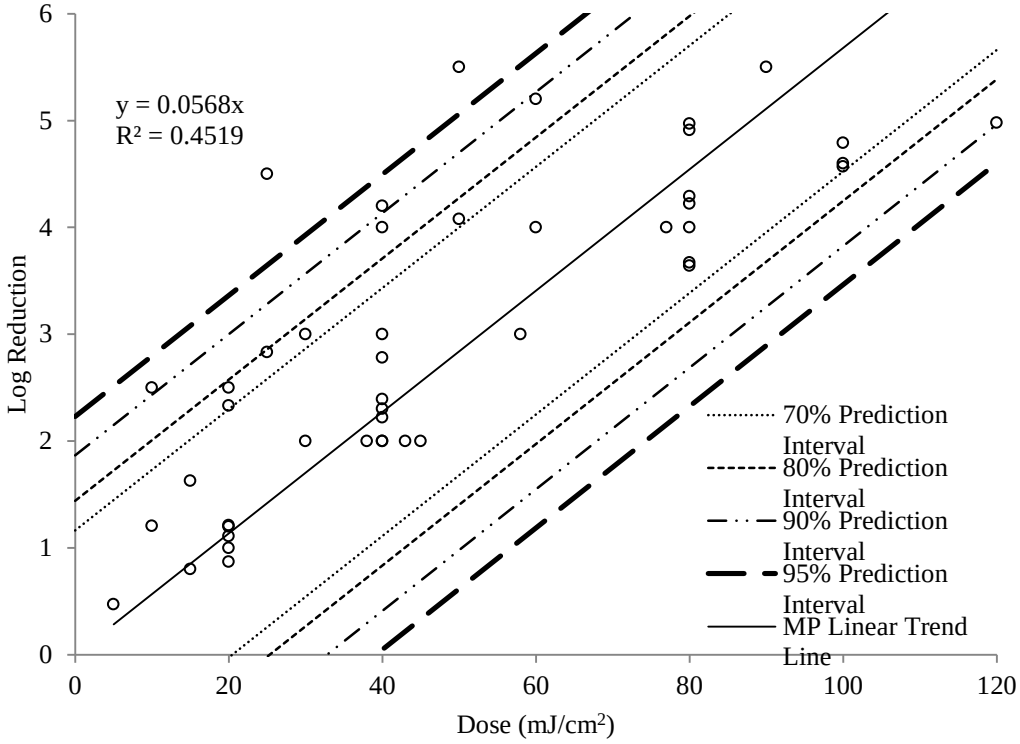

Figure 3-2: MP UV adenovirus inactivation data with prediction intervals

The prediction intervals shown above further strengthen the confidence in MP UV inactivation of adenovirus. They suggest 4-log reduction of adenovirus is achievable with much lower doses of MP UV irradiation compared to LP UV even at high confidence levels. Table 3-2 shows the prediction intervals required for 1, 2, 3, and 4-log reduction of adenovirus using the MP UV compilation data to further elucidate necessary dosing requirements for MP UV irradiation.

Table 3-2: Lists prediction intervals for UV doses required for 1-, 2-, 3-, and 4-log reduction of adenovirus

Log Reduction	70% Prediction Interval	80% Prediction Interval	90% Prediction Interval	95% Prediction Interval
1	-2.88 - **38.02**	-7.77 - **42.89**	-15.28 - **50.37**	-21.68 - **56.76**
2	14.75 - **55.60**	9.87 - **60.47**	2.36 - **67.95**	4.05 - **74.33**
3	32.39 - **73.17**	27.50 - **78.04**	20.00 - **85.52**	13.59 - **91.91**
4	50.03 - **90.75**	45.14 - **95.62**	37.63 - **103.09**	31.23 - **109.48**

Based on this data compilation and analysis, even at high confidence levels, 95%, MP UV only requires slightly over 100 mJ/cm^2 for 4-log reduction at the upper portion of the interval. So even at the upper end of the highest confidence level analyzed, the dose required for 4-log reduction of the virus by MP UV is around 80 mJ/cm^2 less than that required by LP UV irradiation.

3.3 Motivation for Protein Research

The data from the recent studies clearly show the increased efficiency of MP UV irradiation over that of LP UV; however, this brings up the question of why adenovirus exhibits increased susceptibility to MP UV lamps. Furthermore, there is also a challenge MP UV systems face involving the low wavelength emission of MP UV lamps.

It is important to understand why MP UV irradiation is highly effective towards adenovirus compared to LP UV. A detailed explanation of UV-induced damage to DNA can be found in Chapter 2. For this section, it is important to note the highest efficiency formation of DNA photoproducts occurs close to the absorption peak at ~260 nm. However, UV-C irradiation has also been shown to cause damage to cellular components other than DNA. There is evidence that the increased susceptibility of adenovirus to MP irradiation stems from increased to damage to cellular components, such as proteins, other than genetic material resulting from the polychromatic emission of MP UV lamps (Eischeid and Linden, 2011). Research has shown that

the DNA of viable adenoviruses is not immune to UV light and exposure results in typical formation of UV-induced photoproducts (Eischeid et al., 2008; Rodríguez et al., 2013). Results have shown that LP UV irradiation provides equivalent DNA damage as MP UV irradiation though slightly greater for LP UV irradiation (Eischeid et al., 2008; Rodríguez et al., 2013). These observations indicate that adenoviral susceptibility is most likely not a result of increased damage to the genetic material of the virus. It has been implicated that adenoviral resistance lies in its ability to efficiently use host machinery to repair damaged DNA (Guo et al., 2010). Polychromatic light allows for increased damage to proteins as they absorb strongly at wavelengths other than 253.7 nm. Therefore, adenoviral protein damage could affect vital processes such as attachment or host machinery utilization.

Another aspect of MP UV irradiation giving trouble to the industry is known as the low-wavelength issue. The problem lies in the low-wavelength emission, <240 nm, in polychromatic emission. At these wavelengths, there are differences in water absorbance and quartz-sleeve absorbance or fouling which are not generally accounted for in typical UV sensors, which are focused on detecting UV at 254 nm. These factors will influence the overall dose required from the UV lamps. The issue is escalated by observations that inactivation of surrogate organisms used in validation testing have shown not to be good representations of inactivation levels of challenge organisms, such as adenovirus and cryptosporidium, at low wavelengths. For adenovirus, the commonly used surrogate MS2 shows a drastically increased inactivation at low-wavelengths compared to adenovirus. Although this is good for MP UV irradiation and adenoviral inactivation, it is still important to understand why this phenomenon is occurring.

The above ideas are the major motivations for the research into the effect of lower wavelengths on the viral inactivation. This research aims to investigate adenoviral protein

damage resulting from single-wavelength irradiations across the UV-C spectrum. From this, we hope to gain insight into whether adenoviral susceptibility to polychromatic light is a result of protein damage and possibly determine which proteins or aspect of the infections cycle is affected. This research will also help to explore on the issue involving differences in adenovirus and MS2 inactivation at low wavelengths aiding in the low-wavelength issue investigation.

3.4 SDS-PAGE Background

Protein damage will be determined via a method known as sodium dodecyl sulfate-polyacrylamide gel electrophoresis (SDS-PAGE). Essentially, this is a method which separates proteins based on molecular weight and allows for quantification. The method used in this research was adapted from the work of Eischeid et al. 2011. The principles and mechanisms of the method will be briefly explained here.

As mentioned above, SDS-PAGE is a method which separates proteins based on molecular weight using an electrical gradient to help proteins migrate through polyacrylamide gel. The protein-containing particles are first pro-treated to clean the particles of contaminants and cleave the disulfide bonds between polypeptides effectively disassembling quaternary structure. Following pre-treatment, sodium dodecyl sulfate (SDS) is added to the protein mixture. SDS is an anionic detergent which will bind to the protein and denature secondary and tertiary polypeptide structure to effectively linearize the polypeptide. The above treatment leaves the linearized polypeptide chain with intact peptide bonds, or leaves the polypeptides in their primary structure. The attachment of SDS also imparts a negative charge to the protein. The protein solution is then injected into a polyacrylamide gel. In this case, the polyacrylamide gel had varying concentration of polyacrylamide organized in levels to create a porosity-based gradient. An electrical current is used to help the proteins migrate towards in the gel towards the

positive end. The expectation is that the intact proteins will migrate through the gel until they the porosity becomes too small to get through. Therefore, the largest proteins will stop migrating first while smaller proteins continue and end their migration farther down the gel. The protein size can then be determined by using a comparison to a protein ladder sample composed of proteins with known molecular weights.

In this research, the gel was stained with a fluorescent dye and quantitation was determined based on strength of signal with a higher fluorescent signal indicating more protein. Therefore, the quantities of intact protein are determined based on the relative amount of an untreated sample. As a result, the method would allow for the determination of the most protein damaging wavelengths in the UV-C spectrum based on the relative quantities of proteins in the treated samples.

3.5 Materials and Methods

3.5.1 Irradiations

Adenovirus suspended in PBS was irradiated using a NT242 series Ekspla laser from the National Institute of Standards and Technology (NIST). The laser is tunable between wavelengths of 210 and 2600 nm. For these experiments, the laser was tuned in the range of 210 to 290 nm. Ideally, the laser emits single wavelengths; however, it was measured to emit 1.1-1.7 nm. Wavelengths for irradiation were chosen at 10 nm increments starting at 210 nm through 290 nm. Adenovirus was irradiated at 40 mJ/cm^2 for every wavelength chosen and 80 mJ/cm^2 for all wavelengths except 210 and 220 nm.

3.5.2 SDS-PAGE Protocol

The method was adapted from Eischeid et al 2010 Briefly 1 mL of adenovirus sample

was added to a 1.5 mL microcentrifuge, 2 μg of aprotinin was added to each sample, 32 μL of 2% sodium deoxycholate was added to the solution and mixed thoroughly to bring the overall mixture to 0.05% sodium deoxycholate and it was left at room temperature for 5-10 minutes. The solution was brought to contain 10% TCA by adding 260 μL of 50% TCA and mixed thoroughly. The mixture was left on ice for two hours. The mixture was then centrifuged at 20,000g for 20 minutes at 4-6°C. The supernatant was removed and the mixture was washed with ice-cold acetone and centrifuged at 20,000g for 20 minutes at 4-6°C. The above washing procedure was repeated and the pellets were left to air dry for 10-20 minutes. The dried pellet was suspended in 20 μL Laemmli buffer complete with 5% beta-mercaptoethanol. The solution was heated at ~95°C for 10 minutes and then briefly centrifuged to collect the mixture at the bottom of the microfuge tube (Rexroad et al., 2003; Eischeid and Linden, 2011)(Eischeid 2009).

A broad-range protein standard was prepared according to the manufacturers recommendations.10 μL of the sample was added to the wells of a 4-20% gradient ReadyGel. The electrophoresis step was performed at 200 V for 45-50 minutes. The gel was fixed in 7% acetic acid/10% methanol solution for 30 minutes at room temperature with gentle agitation and then allowed to stain overnight also at room temperature with gentle agitation. The stain used was SYPRO Ruby protein gel stain. The gel was destained in 7% acetic acid/10% methanol solution for 30 minutes at room temperature. The gel was imaged using GelDoc and the image was analyzed using QuantityOne software (Eischeid 2009).

3.6 Results and Discussion

At the time of writing this report, the results have been few and more general and broad than the research is aiming for. Initially, we were attempting to obtain adenovirus samples that were exposed to essentially single-wavelength exposures using the NIST laser. We did indeed

receive these samples and adequate amounts of them; however, the samples were determined to be unusable for SDS-PAGE. Images of the treated gels after the SDS-PAGE procedure are shown in Figure 3-3. It is easy to see that the lanes are completely saturated with protein signal. It is suspected that this protein was an artifact of the propagation procedure and there was a significant enough amount to completely overwhelm the possibility of investigating the adenoviral protein damage. The protein contamination is most likely fetal bovine serum (FBS) which is a common reagent in the propagation of virus. Further, SDS-PAGE of adenoviral proteins requires a significant initial concentration (~10^8 PFU/ml) and as a result, dilution of the sample did not remedy the situation.

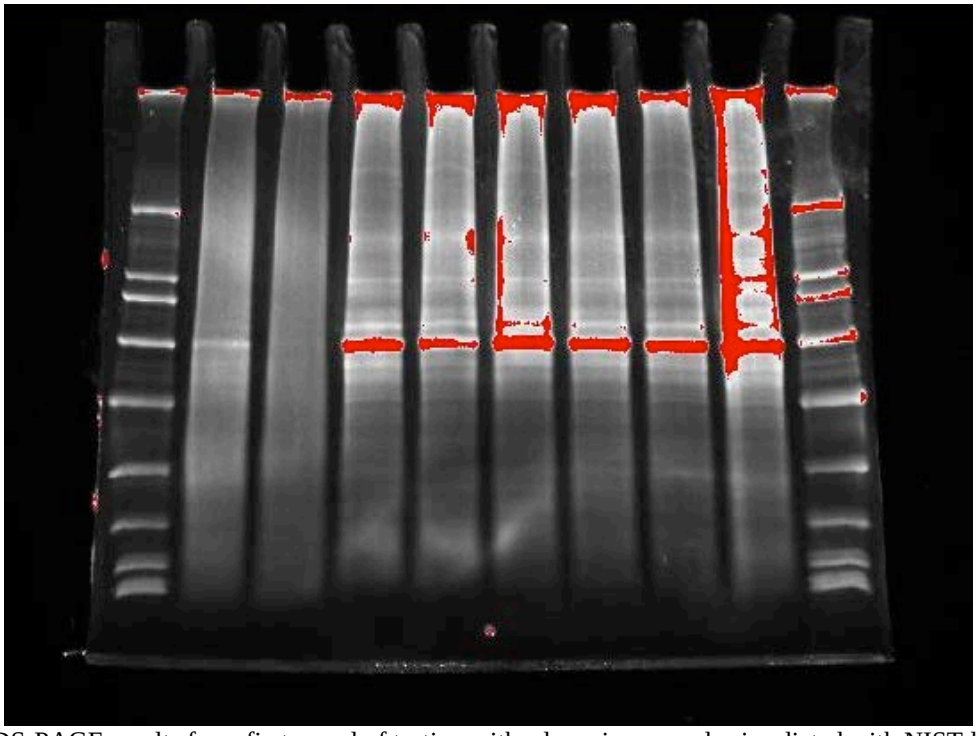

Figure 3-3: SDS-PAGE results from first round of testing with adenovirus samples irradiated with NIST laser

We obtained another sample of treated adenovirus after another round of testing. With this sample, steps were taken during the propagation procedure to eliminate the presence of the

contaminating protein. SDS-PAGE was performed and the resulting images are shown in Figure 14**.** Since there was a limited amount of treated samples, they were diluted to $10^{7.5}$ PFU/mL. The protein signatures came out much cleaner this round; however, there is still a lot of interference and analysis to determine protein quantity was difficult. Furthermore, there appears to be a large protein signature from FBS at 66kD present in most samples. However, there also appears to be other protein signals present in the lanes that are most likely from adenovirus and there is valuable information that can be taken away from these samples, even though quantification was unable to be determined.

Figure 3-4(a) shows the protein signatures from adenovirus that was untreated (Lane 2) and exposed to 210, 220, 230, and 253.7 nm. The irradiations for 230 nm and 253.7 nm were performed using two different doses. Figure 3-4(b) shows adenovirus exposed to higher wavelengths in the UV-C spectrum including 240, 260, 270, and 280 nm at two different doses. The results indicate that at lower wavelengths, protein signatures are much weaker and completely cleared in some cases. This observation suggests that lower wavelengths denature and destroy adenoviral proteins.

a.)

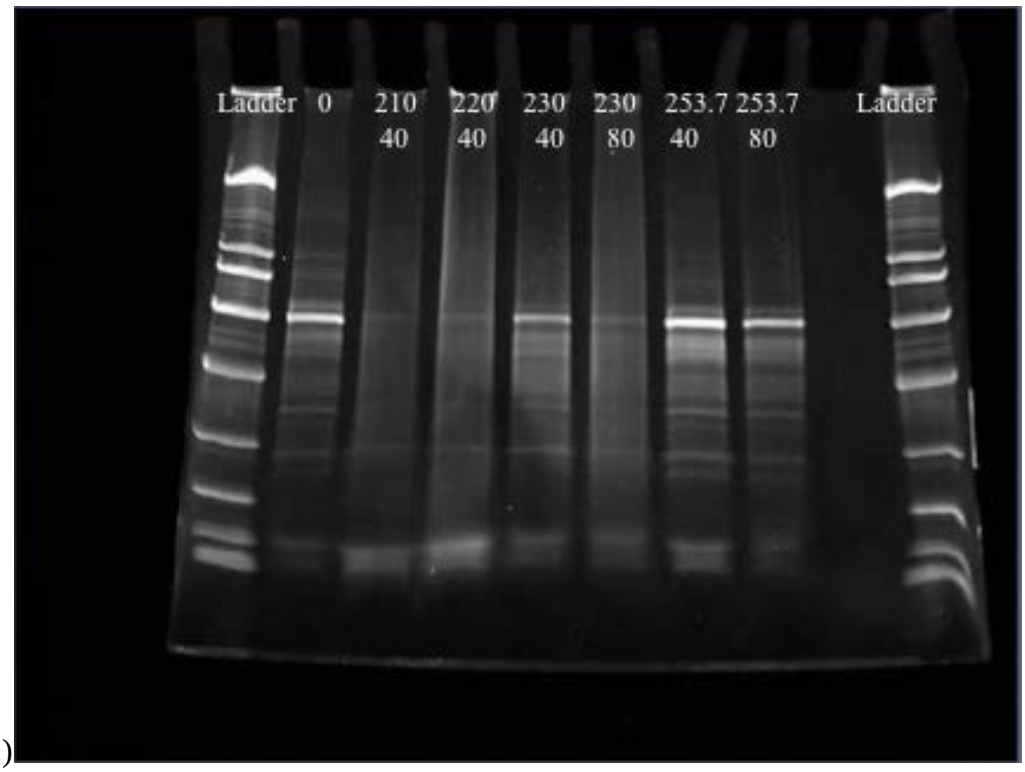

b.)

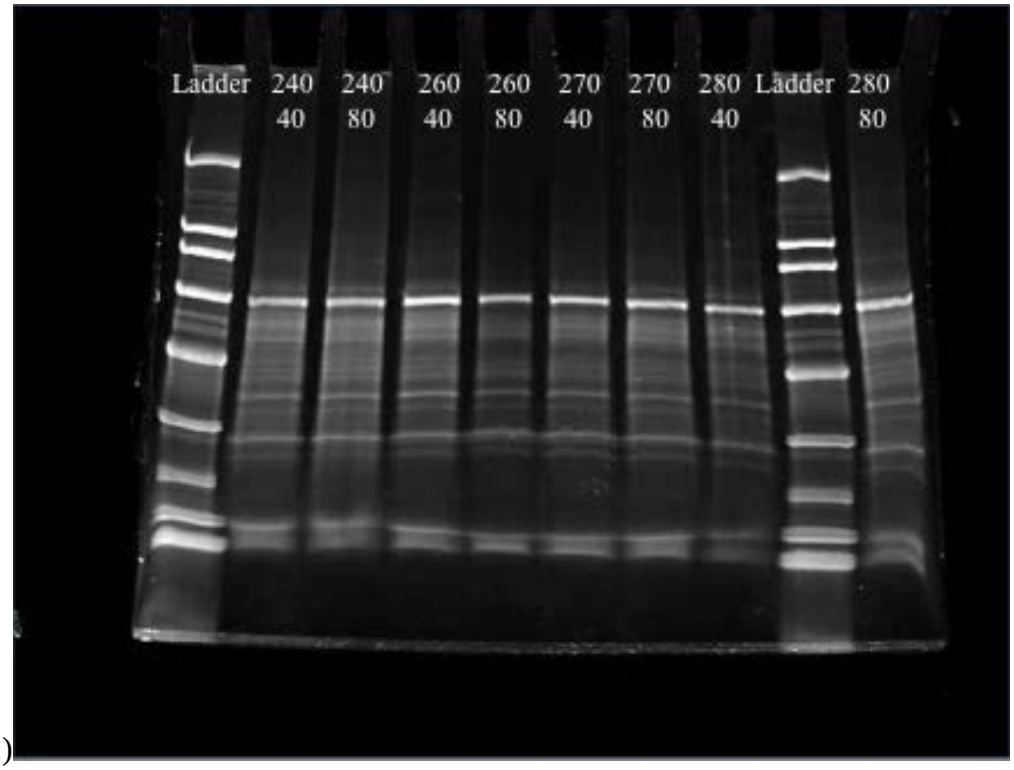

Figure 3-4: Image of SDS-PAGE analysis. Images contain different samples with varying wavelengths and dose. Lanes are labeled with wavelength (top number) and UV dose (bottom number in mJ/cm^2).

3.7 Conclusions and Future Work

Several speculative conclusions can be formed from these observations. The increased protein damage at lower wavelengths could help to explain the increased susceptibility seen at lower wavelengths in the adenoviral action spectra compared to other viral action spectras such as MS2. Furthermore, this observation could help to explain the increased susceptibility of adenovirus to MP UV irradiation compared to LP UV irradiation. Adenoviral proteins are heavily involved in the infection cycle aiding in attachment, host cell utilization, and viral DNA replication. When damaged by the lower wavelength emission present in MP UV irradiation, the proteins may lose function and decrease viability of the virus.

Currently, there is research underway to resolve the clarity of the images and obtain more quantitative results. We are continuing to analyze the samples irradiated using the NIST laser and will also use bandpass filters with an MP UV lamp to irradiate more adenovirus at specified wavelengths and doses. The initial results suggest interesting conclusions and more research is necessary to confidently confirm the results.

References

Battigelli, D,A., Sobsey, M.D., & Lobe, D.C. **1993**. The Inactivation of hepatitis A virus and other model viruses by UV irradiation. *Water Science & Technology*, 27(3-4): 339–42.

Bewley, M.C. **1999** Structural Analysis of the Mechanism of Adenovirus Binding to Its Human Cellular Receptor, CAR. *Science*, 286(5444):1579–83.

Bolton, J.R., Linden, K.G. **2003** Standardization of Methods for Fluence (UV dose) Determination in Bench-scale UV Experiments. *Journal of Environmental Engineering*,129(3): 209–15.

Cadet ,J., Sage, E., Douki, T. **2005.** Ultraviolet Radiation-Mediated Damage to Cellular DNA. *Mutation Research/Fundamental and Molecular Mechanisms of Mutagenesis*. 571(1-2): 3–17.

Crabtree, K.D., Gerba, C.P., Rose, J.B., Haas, C.N. **1997**. Waterborne adenovirus: a risk assessment. *Water Science & Technology*. 35(11): 1–6.

Eischeid, A.C., Linden, K.G. **2007**. Efficiency of Pyrimidine Dimer Formation in Escherichia coli Across UV Wavelengths. *Journal of Applied Microbiology*. 103(5): 1650–6.

Eischeid, A.C., Linden, K.G. **2011**. Molecular Indications of Protein Damage in Adenoviruses after UV Disinfection. *Applied and Environmental Microbiology*. 77(3): 1145–7.

Eischeid, A.C., Meyer, J.N., Linden, K.G. **2008**. UV Disinfection of Adenoviruses: Molecular Indications of DNA Damage Efficiency. *Applied and Environmental Microbiology*. 75(1): 23–8.

Eischeid, A.C., Thurston, J.A., Linden, K.G. **2011**. UV Disinfection of Adenovirus: Present State of the Research and Future Directions. *Critical Reviews in Environmental Science and Technology*. 2011 Aug.;41(15):1375–96.

Eishceid A.C. **2009**. Fundamental Mechanisms in the Extreme UV Resistance of Adenovirus. Department of Civil and Environmental Engineering: Duke University.

Greber, U.F., Willetts, M., Webster, P., Helenius, A. **1993**. Stepwise dismantling of adenovirus 2 during entry into cells. *Cell*, 75(3): 477–86.

Guo, H., Chu, X., Hu, J. **2010**. Effect of Host Cells on Low- and Medium-Pressure UV Inactivation of Adenoviruses. *Applied and Environmental Microbiology*. 76(21): 7068–75.

Guo, M., Hu, H., Bolton, J.R., El-Din, M.G. **2009**. Comparison of Low- and Medium-Pressure Ultraviolet Lamps: Photoreactivation of Escherichia coli and Total Coliforms in Secondary Effluents of Municipal Wastewater Treatment Plants. *Water Research.* 43(3): 815–21.

Johns, H.E., Pearson, M.L., LeBlanc, J.C., Helleiner, C.W. **1964**. The Ultraviolet Photochemistry of thymidylyl-(3′→5′)-thymidine. *Journal of Molecular Biology*. 9(2): 503–IN1.

Johns, H.E., Rapaport, S.A., Delbrück, M. **1962**. Photochemistry of Thymine Dimers. *Journal of Molecular Biology*. 4(2): 104–14.

Linden, K.G., Shin, G.A., Lee, J.K., Scheible, K., Shen, C., Posy, P. **2009**. Demonstrating 4-log Adenovirus Inactivation in a Medium-Pressure UV Disinfection Reactor. *Journal American Water Works Association*. 101(4): 90.

Linden, K.G., Thurston, J., Schaefer, R., Malley, J.P. **2007**. Enhanced UV Inactivation of Adenoviruses under Polychromatic UV Lamps. *Applied and Environmental Microbiology*. 73(23): 7571–4.

Linden, K.G., Salveson, A.T., Thurston, J. **2011**. "Study of Innovative Treatments for Reclaimed Water." *WateReuse Research Foundation.* Product Number 02-009-1. ISBN: 978-1-934183-54-0

Moné, M.J., Volker, M., Nikaido, O., Mullenders, L.H., van Zeeland, A.A., Verschure, P.J. **2011** Local UV-induced DNA Damage in Cell Nuclei Results in Local Transcription Inhibition. *Nature Publishing Group*, 2(11): 1013–7.

Oguma, K., Katayama, H., Ohgaki, S. **2002.** Photoreactivation of Escherichia coli after Low- or Medium-Pressure UV Disinfection Determined by an Endonuclease Sensitive Site Assay. *Applied and Environmental Microbiology*. 68(12): 6029–35.

Pan, Z., Chen, J., Schreier, W.J., Kohler, B., Lewis, F.D. **2012**. Thymine Dimer Photoreversal in Purine-Containing Trinucleotides. *Journal of Physical Chemistry: B.* 116(1): 698–704.

Rastogi, R.P., Richa, K. A., Tyagi, M.B., Sinha, R.P. **2010**. Molecular Mechanisms of Ultraviolet Radiation-Induced DNA Damage and Repair. *Journal of Nucleic Acids.* (6551): 1–32.

Ravanat, J.L., Douki, T., Cadet, J. **2001**. Direct and Indirect Effects of UV Radiation on DNA and its Components. *Journal of Photochemistry and Photobiology B: Biology*. 63(1): 88–102.

Rexroad, J., Wiethoff, C.M., Green, A.P., Kierstead, T.D., Scott, M.O., Middaugh, C.R. **2003**. Structural Stability of Adenovirus Type 5. *Journal of Pharmaceutical Sciences*. 92(3): 665–78.

Rodríguez, R.A., Bounty, S., Linden, K.G. **2013**. Long-range Quantitative PCR for Determining Inactivation of Adenovirus 2 by Ultraviolet Light. *Journal of Applied Microbiology*. 114(6): 1854-65.

San Martín, C. **2012** Latest Insights on Adenovirus Structure and Assembly. *Viruses*. 4(12): 847–77.

Schreiner, S., Martinez, R., Groitl, P., Rayne, F., Vaillant, R., Wimmer, P. **2012**. Transcriptional Activation of the Adenoviral Genome Is Mediated by Capsid Protein VI. *PLoS Pathog*. 8(2).

Setlow, R.B., Carrier, W.L. **1963**. Idenitification of Ultraviolet-Induced Thymine Dimers in

DNA by Absorbance Measurments. *Photochemistry and Photobiology*. 2(1): 49–57.

Setlow, R.B., Setlow, J.K. **1962**. Evidence that Ultraviolet-Induced Thymine Dimers in DNA Cause Biological Damage. *Proceedings of the National Academy of Sciences of the United States of America*. 48(7): 1250.

Shin, G.A., Lee, J.K., Linden, K.G. **2009**. Enhanced Effectiveness of Medium-Pressure Ultraviolet Lamps on Human Adenovirus 2 and its Possible Mechanism. *Water Science & Technology*. 260(4): 851.

Shin, G.A., Linden, K.G., Sobsey, M.D. **2004.** Low-Pressure Ultraviolet Inactivation of Pathogenic Enteric Viruses and Bacteriophages. *Journal of Environmental Engineering and Science*. 4(S1):S7–S11.

Sinha, R.P., Häder, D.P. **2002**. UV-Induced DNA Damage and Repair: a Review. Photochemistry and Photobiology Science. 1(4): 225–36.

Yates, M.V., Malley, J., Rochelle, P., Hoffman, R. **2006**. Effect of Adenovirus Resistance on UV Disinfection Requirements: a Report on the State of Adenovirus Science. *Journal American Water Works Association*. 98(6): 93–106.

Zimmer, J.L., Slawson, R.M. **2002**. Potential Repair of Escherichia coli DNA following Exposure to UV Radiation from Both Medium- and Low-Pressure UV Sources Used in Drinking Water Treatment. *Applied and Environmental Microbiology*. 68(7): 3293–9.

U.S. Environmental Protection Agency. 2006a. UV disinfection guidance manual. EPA 815-D-03-007. Office of Water, U.S. Environmental Protection Agency, Washington, DC.

U.S. Environmental Protection Agency. 2006b. National primary drinking water regulations: the Long Term 2 Enhanced Surface Water Treatment rule. EPA-HQ-OW-2002-0039. Office of Water, U.S. Environmental Protec- tion Agency, Washington, DC.

U.S. Environmental Protection Agency. 2006c. National primary drinking water regulations: the Groundwater Rule. EPA-HQ-OW-2002-0061. Office of Water, U.S. Environmental Protection Agency, Washington, DC.

A. Appendix

A-1. MS2

Bacteriophage MS2 was used to investigate direct CPD reversal in the same way as *E. coli* but to a lesser extent. MS2 has an RNA genome compared to the DNA genome of *E. coli*. RNA has a slightly different composition and chemical structure than DNA, including a nucleobase switch from thymine in DNA to uracil in RNA. Infectivity assays and qPCR trials were performed on the samples.

MS2 Infectivity Assays

Briefly, infectivity assays were performed using subsequent irradiations at 280 nm followed by 240 nm. Initial doses of 280 nm irradiation were 100 mJ/cm^2 and 60 mJ/cm^2 and the results are shown in Figure A-1.

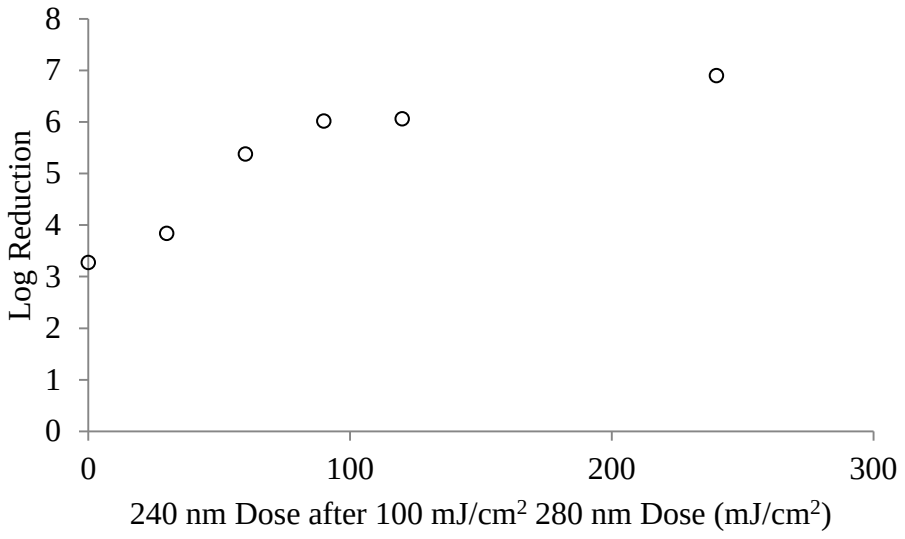

a.)

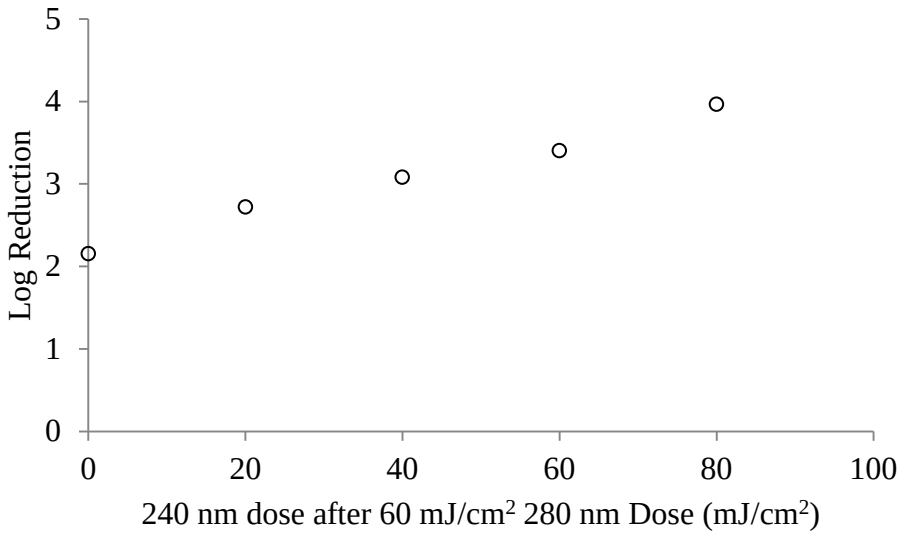

b.)

Figure A-1: MS2 infectivity assays with varying doses of 240 nm irradiation following initial 280 nm irradiation of a.) 100mJ/cm^2 and b.) 60 mJ/cm^2. The x-axis shows subsequent 240 nm doses with a dose of 0 indicating the log reduction from initial 280 nm exposure

Figure A-1 above show log reduction of MS2 after varying doses of 240 nm irradiation following either 100 or 60 mJ/cm^2 of 280 nm irradiation. There is no evidence that there is a slowdown in inactivation due to 240 nm irradiation for either initial dose of 280 nm.

MS2 qPCR:

qPCR was performed on MS2 RNA extracted from samples that were initially exposed to 110 mJ/cm^2 and subsequently exposed to varying doses of 230 nm irradiation. Two fragment sizes were used with lengths 388 and 1184 base pairs. The results are shown in Figure A-2.

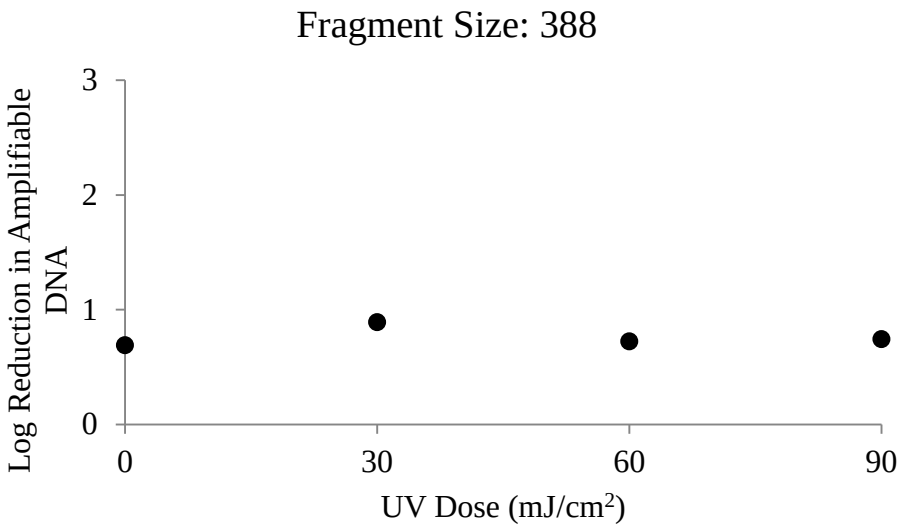

a.)

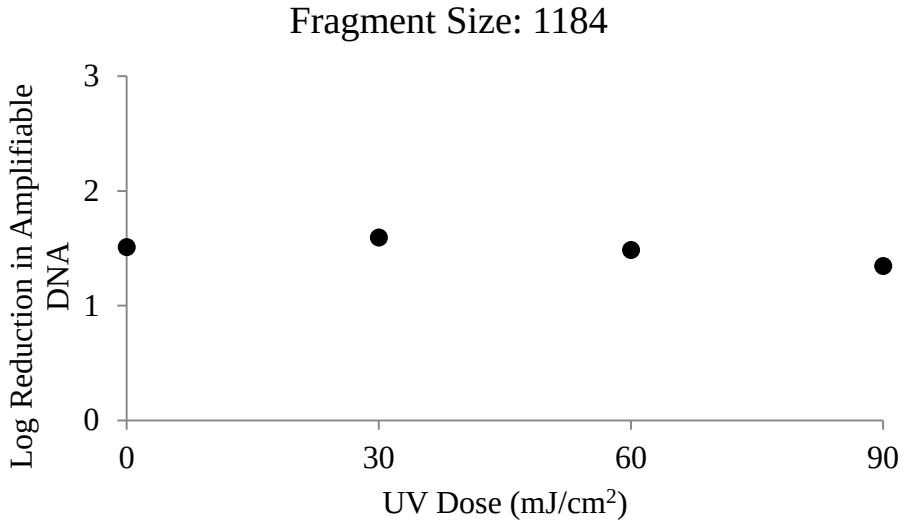

b.)

Figure A-2: qPCR results showing log reduction of amplifiable RNA using fragment sizes a.) 388 bp and b.) 1184 bp. The x-axis shows subsequent 230 nm doses with a dose of 0 indicating the log reduction from initial 280 nm exposure (110 mJ/cm^2).

The fragment sizes analyzed by qPCR showed essentially no increase or decrease in amplifiable DNA detection. It is important to note that untreated samples were quantified at about $10^{3\text{-}4}$ PFU/mL when the target initial concentration was closer to $10^{6\text{-}7}$ PFU/mL. This could indicate that the primer sets were not ideal for MS2; however, there is no indication that 230 nm irradiation has a damage-reversing or damage-inducing effect on

RNA.

A-2. CPD ELISA

An enzyme-linked immunosorbent assay (ELISA) is a method using antibodies specific for certain compounds or ligands that allows for quantification of that compound or ligand. An ELISA specific for CPDs was performed on some *E. coli* DNA samples used in the qPCR experiments explained earlier in this thesis. Only the results are shown for Design 1 samples only including the single-wavelength controls. The two different exposures are both shown as a way to illustrate the variability in the results. The results are shown in Figure A-3

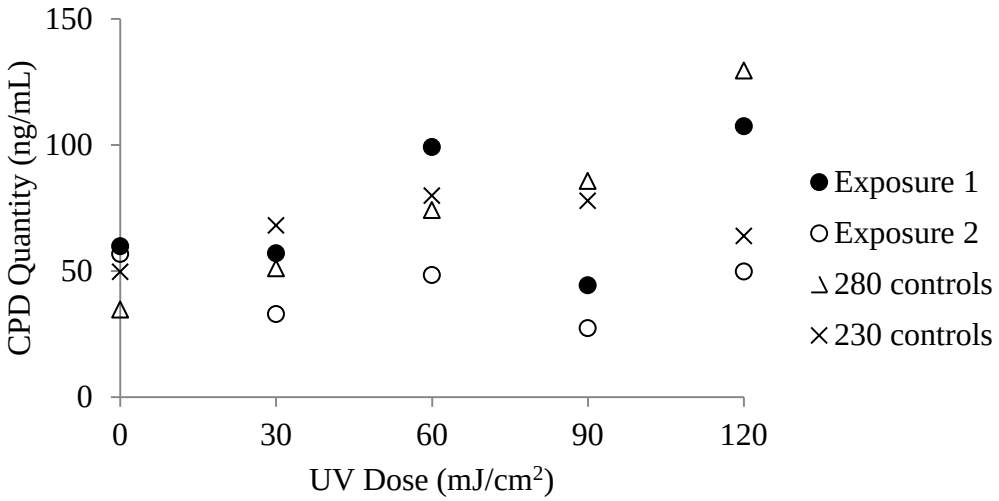

a.)

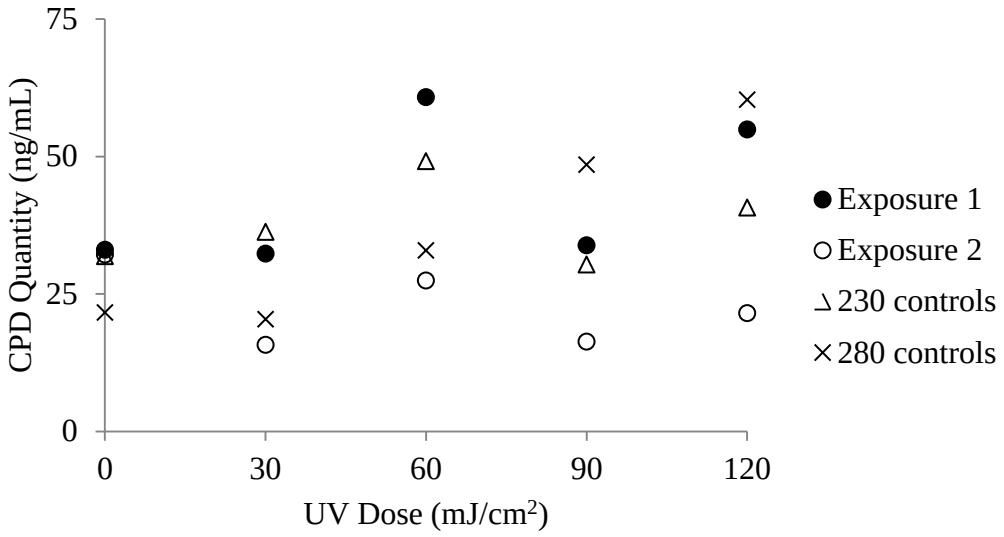

b.)

Figure A-3: CPD quantification using ELISA for Design 1 samples for tow different ELISA trials (a. and b.). The x-axis shows subsequent 230 nm doses with a dose of 0 indicating the log reduction from initial 280 nm exposure (120 mJ/cm^2).

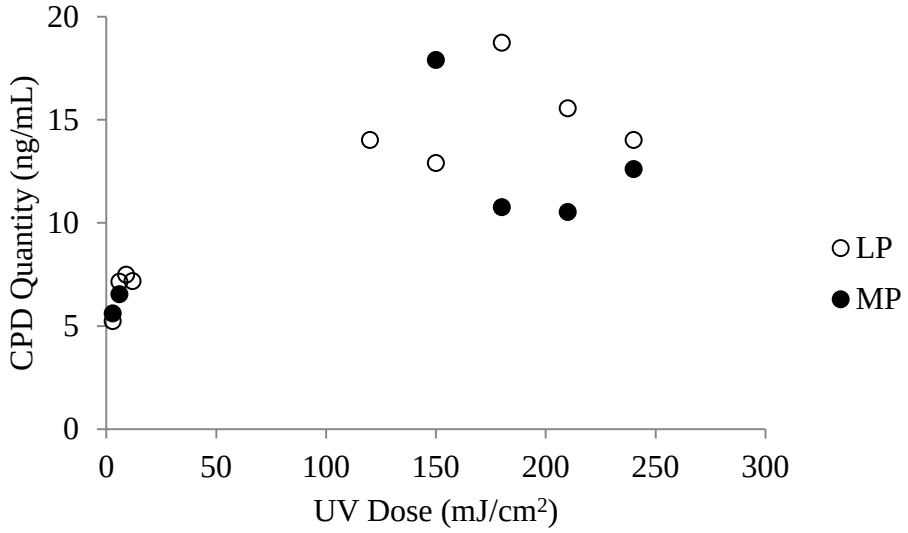

Figure A-4: Attempt to create dose response for CPD formation of MP and LP irradiation. X-axis shows UV dose.

The results are extremely varied and demonstrated a significant difference in the amount of CPDs detected between ELISA trials. Furthermore, the ELISA method was performed on samples exposed to only LP or MP irradiation as an attempt to evaluate efficacy and determine a

dose-response curve (Figure A-4). The results showed a lot of variation in the dose-response deviating from the expectation of a more linear representation. Also, the results indicate that MP and LP irradiation resulted in significantly fewer concentrations of CPDs than 280 and 230 nm irradiations, which is an incorrect assessment. Therefore, the method's efficacy was considered questionable and the results were not used.